

AD777843



Reproduced From
Best Available Copy

Unclassified

SECURITY CLASSIFICATION OF THIS PAGE (When Data Entered)

REPORT DOCUMENTATION PAGE		READ INSTRUCTIONS BEFORE COMPLETING FORM
1. REPORT NUMBER GEP/PH/74-9	2. GOVT ACCESSION NO.	3. RECIPIENT'S CATALOG NUMBER AD 277843
4. TITLE (and Subtitle) DETERMINATION OF REFRACTIVE INDEX OF THIN FILMS FROM INTERFERENCE - FRINGE REFLECTION SPECTRA		5. TYPE OF REPORT & PERIOD COVERED MS Thesis
7. AUTHOR(s) Jan B. Jaeger Captain, USAF		6. PERFORMING ORG. REPORT NUMBER
9. PERFORMING ORGANIZATION NAME AND ADDRESS Air Force Institute of Technology Air University Wright-Patterson AFB, Ohio 45433		8. CONTRACT OR GRANT NUMBER(s)
11. CONTROLLING OFFICE NAME AND ADDRESS Laser Window Division (AFML/LPL) Air Force Materials Laboratory Wright-Patterson AFB, Ohio 45433		10. PROGRAM ELEMENT, PROJECT, TASK AREA & WORK UNIT NUMBERS
14. MONITORING AGENCY NAME & ADDRESS (if different from Controlling Office)		12. REPORT DATE March 1974
		13. NUMBER OF PAGES 92
		15. SECURITY CLASS. (of this report) Unclassified
		15a. DECLASSIFICATION/DOWNGRADING SCHEDULE
16. DISTRIBUTION STATEMENT (of this Report) Approved for public release; distribution unlimited.		
17. DISTRIBUTION STATEMENT (of the abstract entered in Block 20, if different from Report) Reproduced by NATIONAL TECHNICAL INFORMATION SERVICE U S Department of Commerce Springfield VA 22151		
18. SUPPLEMENTARY NOTES Approved for public release; IAW AFR 190-17 <i>Jerry C. Hix</i> Jerry C. Hix, Captain, USAF Director of Information		
19. KEY WORDS (Continue on reverse side if necessary and identify by block number.) Index of Refraction of Thin Films Cadmium Selenide Reflection Spectra Cadmium Telluride Laser Window Coating Germanium Cadmium Sulfide Zinc Sulfide		
20. ABSTRACT (Continue on reverse side if necessary and identify by block number) Reflection spectra were recorded on selected thin film materials from 2.5 μ to 17.0 μ using light polarized parallel to the plane of incidence. The materials were CdS, CdSe, CdTe, Ge, ZnS, ZnSe, and ZnTe vacuum evaporated onto KCl substrates. The spectra were analyzed using two different techniques: (1) The Fresnel reflection coefficients were applied to a three media model, where the second medium had an extinction coefficient, and (2) an index of refraction was computed from the interference fringes of the spectra.		

DD FORM 1 JAN 73 1473

EDITION OF 1 NOV 65 IS OBSOLETE

Unclassified

SECURITY CLASSIFICATION OF THIS PAGE (When Data Entered)

Unclassified

SECURITY CLASSIFICATION OF THIS PAGE(When Data Entered)

Block 19 (Key Words) (Continued)

Zinc Selenide
Zinc Telluride
Potassium Chloride Substrate

Block 20 (Abstract) (Continued)

The interference-fringe analysis indicates that the index of refraction of the thin film coatings is approximately the same as that of the bulk material in the 10.0 micron region, except for CdS.

Approved for public release; LA 484 190-17

James G. Smith, Captain, USAF
Director of Information

Unclassified

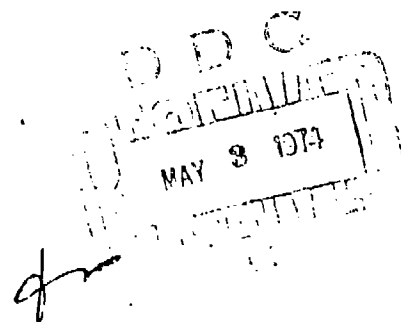
SECURITY CLASSIFICATION OF THIS PAGE(When Data Entered)

DETERMINATION OF REFRACTIVE INDEX
OF THIN FILMS FROM INTERFERENCE-
FRINGE REFLECTION SPECTRA

THESIS

GEP/PH/74-9

JAN B. JAEGER
CAPTAIN, USAF



Approved for Public Release; Distribution Unlimited

ib

DETERMINATION OF REFRACTIVE INDEX OF THIN
FILMS FROM INTERFERENCE - FRINGE REFLECTION SPECTRA

THESIS

Presented to the Faculty of the School of Engineering
of the Air Force Institute of Technology

Air University

In Partial Fulfillment of the
Requirements for the Degree of
Master of Science

by

Jan B. Jaeger, B.S.C.E.
Captain USAF

Graduate Engineering-Physics

January, 1974

Approved for Public Release; Distribution Unlimited

ic

Preface

This thesis is an in-house project conducted under the guidance of the Laser Window Branch of the Air Force Materials Laboratory.

I would like to thank Major Kenneth C. Jungling for serving as thesis advisor. He helped me overcome numerous obstacles encountered during this study. A special thanks goes to Dr. G. T. Johnston and Mr. John R. Fenter. Their encouragement, assistance, and sense of humor were invaluable aids as this study progressed, and sometimes digressed. Thanks also go to Mr. Pat Larger whose technical assistance and "crank it up" philosophy were always a welcome aid. A thank you is also due to the remaining members of the Laser Window Branch, without whose help this thesis would never have been completed.

A most special thank you goes to my wife, Diane. Her encouragement, patience, and interest were the ultimate factor in completing this thesis.

Jan B. Jaeger

Contents

	Page
Preface	ii
List of Figures	iv
List of Tables	v
Abstract	vii
I. Introduction	1
II. Theory	4
Introduction	4
Derivation and Use of Total Reflectance Expression	6
Interference Fringe Analysis	14
III. Experimental Samples, Equipment, Problems, Procedure, and Parameters	17
Introduction	17
Samples	17
Apparatus	18
Experimental Problems	22
Optical Alignment	22
Light Spillover	23
Sample and Reference Mirror Mounts	23
Experimental Procedure	24
Parameters	25
IV. Results and Conclusions	27
Introduction	27
Experimental Spectra	27
Total Reflectance Analysis	32
Interference Fringe Analysis	34
Bulk vs Thin Film Index	37
V. Recommendations	39
Bibliography	40
Appendix A: Condition of Coatings	43
Appendix B: Table of Normalized Experimental Reflectances	45
Appendix C: Tables of Maxima and Minima in the Reflection Spectra	62
Appendix D: Computed Indices of Refraction	70
Appendix E: Flow Chart of Computer Program	78
VITA	80

List of Figures

Figure		Page
1	Three Media Model Used In Total Reflectance Analysis	6
2	Intersection of n_2 vs k_2 Curves	12
3	Two-Media Model Used to Determine the Refractive Index of the Substrate	13
4	Three Media Model Used In Interference Fringe Analysis.	14
5	View of Both Sides of a Coated Blank	17
6	Attachment Placement and Beam Paths	19
7	Sample Unit	20
8	Reflection Spectrum for 22° Incident Angle	29
9	Reflection Spectrum for 51° Incident Angle	30
10	Reflection Spectrum for 63° Incident Angle	31
11	Wavenumber Difference Between Fringes for CdSe	36
12	Indices of Refraction In 10.0μ Region	37
13	Flow Chart of Computer Program	81

List of Tables

Table		Page
I	Table of Normalized Experimental Reflectances for Zinc Sulfide, 2.71 Microns	47
II	Table of Normalized Experimental Reflectances for Zinc Sulfide, 2.65 Microns	48
III	Table of Normalized Experimental Reflectances for Germanium, 1.27 Microns	49
IV	Table of Normalized Experimental Reflectances for Germanium, 1.33 Microns	50
V	Table of Normalized Experimental Reflectances for Cadmium Selenide, 2.41 Microns	51
VI	Table of Normalized Experimental Reflectances for Cadmium Selenide, 2.59 Microns	52
VII	Table of Normalized Experimental Reflectances for Cadmium Telluride, 2.06 Microns	53
VIII	Table of Normalized Experimental Reflectances for Cadmium Telluride, 2.09 Microns	54
IX	Table of Normalized Experimental Reflectances for Zinc Selenide, 2.06 Microns	55
X	Table of Normalized Experimental Reflectances for Zinc Selenide, 2.03 Microns	56
XI	Table of Normalized Experimental Reflectances for Zinc Telluride, 1.71 Microns	57
XII	Table of Normalized Experimental Reflectances for Zinc Telluride, 1.74 Microns	58
XIII	Table of Normalized Experimental Reflectances for Cadmium Sulfide, 1.80 Microns	59
XIV	Table of Normalized Experimental Reflectances for Cadmium Sulfide, 1.83 Microns	60
XV	Table of Normalized Experimental Reflectances for Potassium Chloride	61

List of Tables

Table		Page
XVI	Table of Reflectance Maxima and Minima for Zinc Sulfide	63
XVII	Table of Reflectance Maxima and Minima for Germanium .	64
XVIII	Table of Reflectance Maxima and Minima for Cadmium Selenide	65
XIX	Table of Reflectance Maxima and Minima for Cadmium Telluride	66
XX	Table of Reflectance Maxima and Minima for Zinc Selenide	67
XXI	Table of Reflectance Maxima and Minima for Zinc Telluride	68
XXII	Table of Reflectance Maxima and Minima for Cadmium Sulfide	69
XXIII	Computed Indices of Refraction for Zinc Sulfide	71
XXIV	Computed Indices of Refraction for Germanium	72
XXV	Computed Indices of Refraction for Cadmium Selenide . .	73
XXVI	Computed Indices of Refraction for Cadmium Telluride. .	74
XXVII	Computed Indices of Refraction for Zinc Selenide . . .	75
XXVIII	Computed Indices of Refraction for Zinc Telluride . . .	76
XXIX	Computed Indices of Refraction for Cadmium Sulfide. . .	77

Abstract

Reflection spectra were recorded on selected thin film materials from 2.5μ to 17.0μ using light polarized parallel to the plane of incidence. The materials were CdS, CdSe, CdTe, Ge, ZnS, ZnSe, and ZnTe vacuum evaporated onto KCl substrates. The spectra were analyzed using two different techniques: (1) the Fresnel reflection coefficients were applied to a three media model, where the second medium had an extinction coefficient, and (2) an index of refraction was computed from the interference fringes of the spectra. The interference fringe analysis indicates that the index of refraction of the thin film coatings is approximately the same as that of the bulk material in the 10.0 micron region, except for CdS.

DETERMINATION OF REFRACTIVE INDEX OF THIN
FILMS FROM INTERFERENCE-FRINGE REFLECTION SPECTRA

I. Introduction

The development of the high power infrared laser has generated a requirement for increasing the transmittance of laser windows. The inherent transmittance of any laser window material is increased by using a multilayer anti-reflection (AR) thin film coating. The design of an AR coating requires accurate knowledge of the optical constants of each thin film material in the wavelength region where it will be used. The optical constants of a material are the real and imaginary parts of the complex index of refraction, $\hat{n} = n + ik$, where n is the true index of refraction and k is the extinction coefficient. The extinction coefficient is directly related to the absorption coefficient, $\alpha = \frac{4\pi k}{\lambda_0}$, λ_0 being the wavelength of incident light in vacuum, and is a measure of how much incident energy will be absorbed by a material (Ref 4:611).

Many thin film materials are currently being developed and used without the optical constants being adequately characterized. The optical constants of some of these materials in bulk form are known in the infrared, but the optical constants of the material used as a thin film are believed to be different from those of the bulk material. In order to satisfactorily design the necessary AR coatings, the optical constants of these materials need to be determined.

Seven proposed thin film AR coating materials were investigated to determine their optical constants. The materials were cadmium

selenide, cadmium sulfide, cadmium telluride, germanium, zinc selenide, zinc sulfide, and zinc telluride. Each material was vacuum evaporated onto a potassium chloride substrate. The samples studied, then, consisted of a thin monolayer coating of each material on a potassium chloride substrate.

The reflection spectra of the samples were recorded from 2.5 to 17.0 microns using a Perkin-Elmer 225 dual beam spectrophotometer with a reflectance attachment. The incident light was polarized parallel to the plane of incidence. Two methods were used to analyze the spectra.

In one method an index of refraction, n , was calculated from the wavenumber spacing between interference fringes in the spectra. This method yielded an average n over the interference fringe or fringes used to calculate n . This method had two disadvantages: (1) an n at a specific wavelength could not be calculated, and (2) this method did not account for an extinction coefficient, k . Therefore, a second method was used to analyze the spectra.

In order to be able to obtain an n and a k at a specific wavelength, the Fresnel reflection coefficients were applied to a two boundary system to derive an expression for the total reflectance of a sample in terms of n and k of the thin film coating and the incident angle of light. A computer program was used to determine simultaneous values of n and k that would yield reflectance values equal to the experimental reflectance values. A number of simultaneous n and k values was determined for each angle. Then for any incident angle, these pairs of n and k would plot a curve on an n vs k diagram. If two incident angles were used, two curves could be plotted. These two

curves should cross at some point which would determine the n and k of the thin film coating. Since the reflectance values used were at a specific wavelength, the determined n and k values would be valid for a specific wavelength.

In order to simplify the equations used to analyze the spectra, the air/film/substrate system was treated as an ideal two boundary system. No attempt was made to account for discontinuities in the coatings, the condition of the substrate, or method of coating preparation. Each of these would have an impact on the analysis of any data.

The remainder of this report is arranged as follows. The theory pertinent to the equations used to analyze the spectra is developed in Chapter II. The experimental apparatus used is described in Chapter III. Experimental problems and procedure are also discussed in Chapter III. The results and conclusions are presented in Chapter IV and some recommendations for improvement are discussed in Chapter V.

II. Theory

Introduction

As mentioned in Chapter I, the reflection spectra were analyzed by two different methods. The theory pertinent to each method will be developed in this chapter. One method was to take the normalized reflectance value at a specific wavelength, and to analytically find the index of refraction and extinction coefficient of the thin film by applying the Fresnel reflection coefficients to a two boundary system. The second method was to compute an index of refraction for the thin film from the reflection spectra interference fringes. Both methods were modeled by a three media system, and the following simplifying assumptions were made:

- a. Only medium two, the thin film coating, had an extinction coefficient.
- b. There was no contribution to the total reflectance from the back surface of the substrate, medium three.
- c. All three media were linear, homogeneous, and isotropic.

The first assumption was based on the following considerations. The beam path lengths for the reference and sample beams were matched. Therefore, any difference in absorption of the two beams by air should be small. At one point in the beam paths, the sample beam was reflected off the sample while the reference beam was reflected off an aluminum reference mirror. At any other time the two beams were reflected off similar surfaces. The difference of absorption between these reflecting surfaces was assumed to be small. In order to simplify the analysis,

the total extinction coefficient for medium 1 was assumed to be zero. Medium three was potassium chloride and its extinction coefficient is much less than one, so its extinction coefficient was also assumed to be zero to simplify the analysis.

The second assumption was not demonstrated to be correct or incorrect by experiment. A spectrum of one of the thin film coatings was recorded at the 51 degree incident angle. Then the back surface of the substrate was thoroughly sandpapered and another spectrum recorded. The two spectra were identical between 2.5 and 5.0 microns, however between 5.0 and 17.0 microns the maximum amplitude of the second spectrum was one to two per cent less than the first spectrum. This might indicate that there was some contribution to total reflectance by the back surface of the substrate. However, a difference of this magnitude also occurred in some of the thin film spectra for equal film thicknesses, so the test was inconclusive. No more tests were run, because each test would destroy one side of a sample.

The third assumption was inaccurate. Only one of the coatings physically appeared to be a good coating. The remainder were scratched and/or fogged, or had run. An individual description of each coating is included in Appendix A. Unfortunately, it was not possible to avoid these imperfections by adjusting the beam position. In numerous substrates one could see sub-surface cracks. The substrates were mechanically polished, so the sub-surface cracks are probably an indication of internal stress.

The remainder of this chapter is divided into two sections. In the first section, the equations used in the normalized reflectance analysis

are derived. In the second section, the equation used to compute the Index of refraction from Interference fringes is derived.

Derivation and Use of Total Reflectance Expression

The thin film coatings were analyzed using the three media model shown in Figure 1, where r_1 and r_2 are the Fresnel reflection coefficients at the air/film interface and the film/substrate interface respectively. The n 's are the indices of refraction of their respective media. θ_1 is the angle of incidence, and θ_2 and θ_3 are the angles of refraction in their respective media.

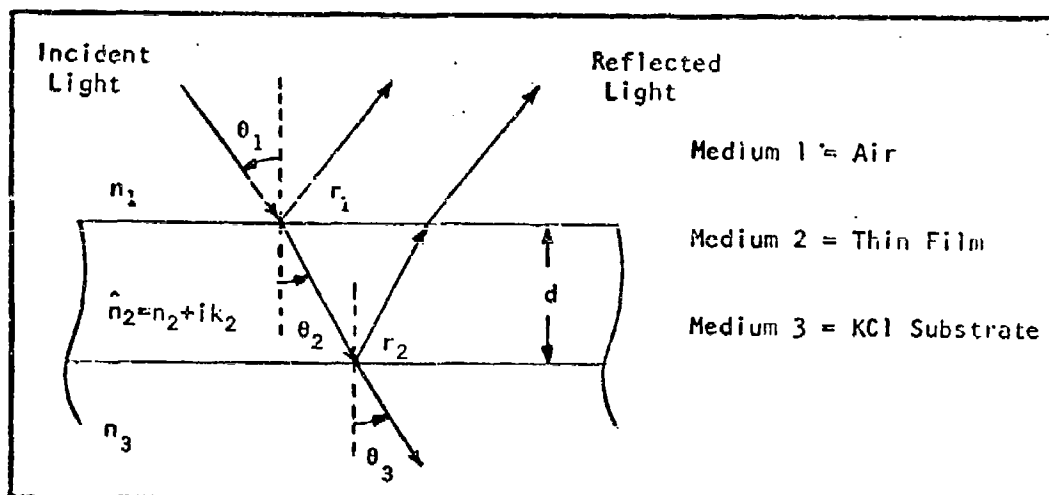


Fig. 1. Three Media Model Used in Total Reflectance Analysis

The index of refraction for the film becomes complex with the addition of an extinction coefficient and is defined as follows:

$$\hat{n}_2 = n_2 + ik_2 \quad (1)$$

where n_2 is the true index of refraction and k_2 is the extinction coefficient.

Now for the sake of mathematical convenience one can make the following definition:

$$\hat{n}_2 \cos \theta_2 = u + iv \quad (2)$$

where $\cos \theta_2$ is a complex quantity.

The fact that $\cos \theta_2$ and $\sin \theta_2$ are complex quantities stem from the laws of Fresnel and Snell which are still valid in a purely formal way (Ref 28:501).

$$\sin \theta_2 = \frac{n_1}{n_2 + ik_2} \sin \theta_1 \quad (3)$$

$$\cos \theta_2 = \sqrt{1 - \left(\frac{n_1}{n_2 + ik_2} \sin \theta_1 \right)^2} \quad (4)$$

The physical interpretation of this has to do with the planes of constant phase and constant amplitude of an electromagnetic wave in a conducting medium, that is a medium with an extinction coefficient. In a pure dielectric (no conductivity), the planes of constant phase and constant amplitude are the same. In a conducting medium such as medium 2 in Figure 1, the planes of constant amplitude are parallel to the air/film interface. The planes of constant phase make some angle ϕ with the planes of constant amplitude. This angle ϕ is the true refraction angle and is a rather complicated function of the incident angle (Ref 28:502). So, while θ_2 is not the true refractive angle in medium 2, $\cos \theta_2$ and $\sin \theta_2$ are complex quantities and can be used in a formal way to derive an expression for total reflectance.

Now square both sides of (2):

$$(\hat{n}_2 \cos \theta_2)^2 = u^2 + 2iuv - v^2 \quad (5)$$

Using Snell's law and $\sin^2 \theta_2 = 1 - \cos^2 \theta_2$, one can get:

$$\hat{n}_2^2 \cos^2 \theta_2 = \hat{n}_2^2 - n_1^2 \sin^2 \theta_1 \quad (6)$$

Combine equations (5) and (6), and equate the real and imaginary parts:

$$u^2 - v^2 = n_2^2 - k_2^2 - n_1^2 \sin^2 \theta_1 \quad (7)$$

$$uv = n_2 k_2 \quad (8)$$

Now, solve equations (7) and (8) simultaneously and apply the quadratic formula:

$$2u^2 = (n_2^2 - k_2^2 - n_1^2 \sin^2 \theta_1) + \sqrt{(n_2^2 - k_2^2 - n_1^2 \sin^2 \theta_1)^2 + 4(n_2 k_2)^2} \quad (9)$$

$$2v^2 = -(n_2^2 - k_2^2 - n_1^2 \sin^2 \theta_1) + \sqrt{(n_2^2 - k_2^2 - n_1^2 \sin^2 \theta_1)^2 + 4(n_2 k_2)^2} \quad (10)$$

The incident light in the experiment was polarized parallel to the Incident plane, so the Fresnel reflection coefficients, r_1 and r_2 , can be written as follows:

$$r_1 = \frac{\hat{n}_2^2 \cos \theta_1 - n_1 \hat{n}_2 \cos \theta_2}{\hat{n}_2^2 \cos \theta_1 + n_1 \hat{n}_2 \cos \theta_2} \quad (11)$$

$$r_2 = \frac{\hat{n}_2 n_3 \cos \theta_2 - \hat{n}_2^2 \cos \theta_3}{\hat{n}_2 n_3 \cos \theta_2 + \hat{n}_2^2 \cos \theta_3} \quad (12)$$

Apply definitions (1) and (2) to equations (11) and (12), perform the indicated operations, and separate into real and imaginary parts:

$$r_1 = \frac{(n_2^2 - k_2^2) \cos \theta_1 - n_1 u + i(2n_2 k_2 \cos \theta_1 - n_1 v)}{(n_2^2 - k_2^2) \cos \theta_1 + n_1 u + i(2n_2 k_2 \cos \theta_1 + n_1 v)} \quad (13)$$

$$r_2 = \frac{-(n_2^2 - k_2^2) \cos \theta_3 + n_3 u + i(-2n_2 k_2 \cos \theta_3 + n_3 v)}{(n_2^2 - k_2^2) \cos \theta_3 + n_3 u + i(2n_2 k_2 \cos \theta_3 + n_3 v)} \quad (14)$$

Now applying the relation $|A| = (AA^*)^{\frac{1}{2}}$, where A^* is the complex conjugate, one gets for $|r_1|$ and $|r_2|$.

$$|r_1| = \left[\frac{(n_2^2 - k_2^2)^2 \cos^2 \theta_1 - 2n_1(n_2^2 - k_2^2) \cos \theta_1 + n_1^2 u^2}{(n_2^2 - k_2^2)^2 \cos^2 \theta_1 + 2n_1(n_2^2 - k_2^2) \cos \theta_1 + n_1^2 u^2} + \frac{4n_2^2 k_2^2 \cos^2 \theta_1 - 4n_2 k_2 n_1 v \cos \theta_1 + n_1^2 v^2}{4n_2^2 k_2^2 \cos^2 \theta_1 + 4n_2 k_2 n_1 v \cos \theta_1 + n_1^2 v^2} \right]^{\frac{1}{2}} \quad (15)$$

$$|r_2| = \left[\frac{(n_2^2 - k_2^2)^2 \cos^2 \theta_3 - 2n_3(n_2^2 - k_2^2) \cos \theta_3 + n_3^2 u^2}{(n_2^2 - k_2^2)^2 \cos^2 \theta_3 + 2n_3(n_2^2 - k_2^2) \cos \theta_3 + n_3^2 u^2} \right. \\ \left. \frac{+ 4n_2^2 k_2^2 \cos^2 \theta_3 - 4n_2 k_2 n_3 v \cos \theta_3 + n_3^2 v^2}{+ 4n_2^2 k_2^2 \cos^2 \theta_3 + 4n_2 k_2 n_3 v \cos \theta_3 + n_3^2 v^2} \right]^{\frac{1}{2}} \quad (16)$$

Apply Snell's law to find $\cos \theta_3$ in terms of θ_1 :

$$\cos \theta_3 = \sqrt{1 - \left(\frac{n_1^2 \sin^2 \theta_1}{n_3^2} \right)^{\frac{1}{2}}} \quad (17)$$

The total amplitude reflection coefficient, r , for this three media system is (Ref 4:61).

$$r = \frac{|r_1| + |r_2| e^{2i\delta}}{1 + |r_1| |r_2| e^{2i\delta}} \quad (18)$$

where

$$\delta = \frac{2\pi}{\lambda} d \hat{n}_2 \cos \theta_2 = 2\pi v d \hat{n}_2 \cos \theta_2 \quad (19)$$

λ is the wavelength of incident light and d is the physical film thickness, and $v = 1/\lambda$ is the wavenumber. The total reflectance, R , will be

$$R = |r|^2 \quad (20)$$

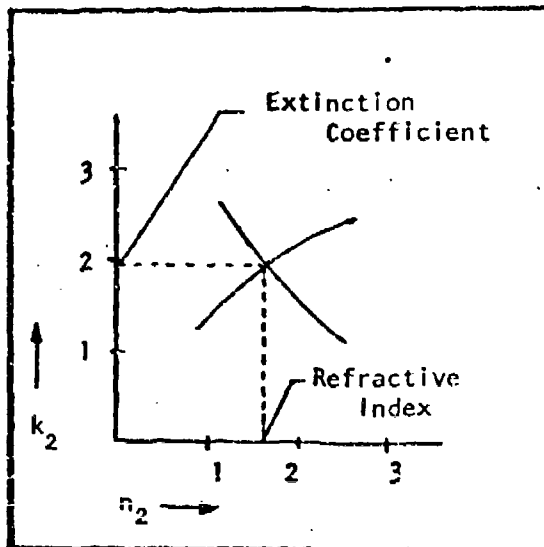
where r is defined in equation (18), and $|r_1|$ and $|r_2|$ are defined in equations (15) and (16), respectively.

This derivation generally follows that of Born and Wolf (Ref 4:624-27). However, there should be no phase interference effects at the spectrophotometer detector due to the extremely short coherence length of the source light and the fact that the area of the detector should be large enough to average out any interference effects. Therefore, a phase relation was not introduced into equations (15), (16), and (18), as Born and Wolf did.

As can be seen from (15), (16), (17), (18), (19), and (20), one needs to know the following variables to compute R ; n_1 , θ_1 , n_2 , k_2 , n_3 , v , d , and $\hat{n}_2 \cos \theta_2$. R and v are determined by the spectrophotometer. The incident angle, θ_1 , and film thickness, d , are measured as explained in the next chapter. The refractive index of air, n_1 , is one, and the refractive index of the substrate, n_3 , can be experimentally determined as shown later. The expression $\hat{n}_2 \cos \theta_2$, was defined as $u + iv$ by (2), and the quantities u and v are expressed in (8) and (9). Thus one knows all the variables in the expression for total reflectance at a specified wavelength except n_2 and k_2 .

At any given wavelength all the measured variables and n_3 will be constant and there will be numerous values of n_2 and k_2 that will satisfy equation (20). However, for any given value of n_2 there will be a unique value of k_2 . If one assumes a range of n_2 values, then there will be a unique corresponding range of k_2 values. These paired values can be plotted as a curve on an n_2 versus k_2 diagram as discussed by numerous authors (Ref 16). If the angle of incidence is changed, R will change, consequently, new values of k_2 will be found for the same

range of n_2 values. These values of n_2 and k_2 can be plotted as another curve on the same n_2 versus k_2 diagram. The point where these two curves cross determines the values of the true index of refraction and extinction coefficient. An example of how this might appear is shown in Figure 2.



A computer program was written to determine a range of values of n_2 and k_2 that would satisfy the experimental data at 10.6 microns. The flow chart is presented in Appendix E. The range of n_2 used in the computer program was $n_b - 0.4 \leq n_2 \leq n_b + 0.6$ where n_b is the refractive index of the bulk material.

Fig. 2. Intersection of n_2 vs k_2 Curves

It was assumed that this range was sufficiently large to cover any changes in the index of refraction caused by the material being used as a thin film. After the values of n_2 and k_2 were determined by computer calculations at each incident angle, the results were plotted and the true index of refraction and extinction coefficient determined by the point where the curves crossed.

It was previously mentioned that refractive index of the substrate could be determined experimentally. The bare potassium chloride

substrate is nothing more than the two media system shown in Figure 3, if one makes use of the assumptions stated in the Introduction to this chapter.

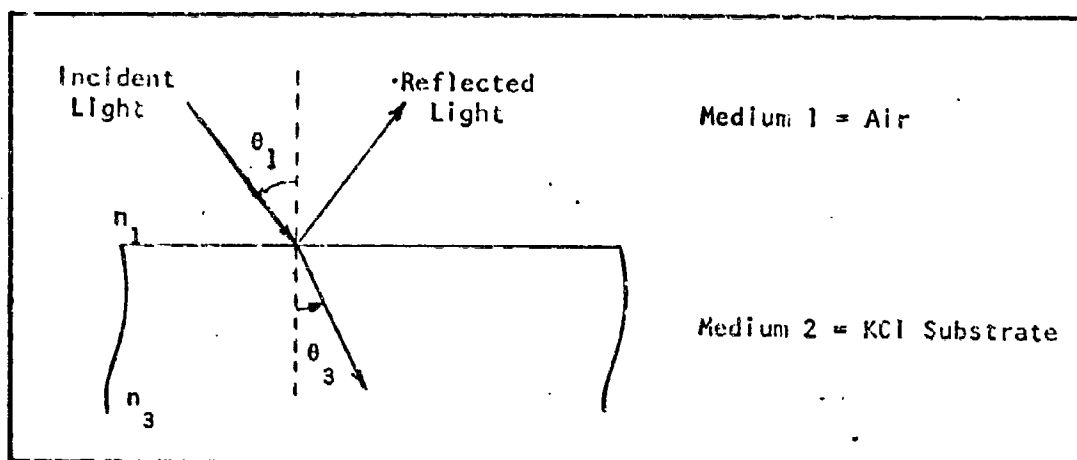


Fig. 3. Two-Media Model Used to Determine the Refractive Index of the Substrate

The incident light is polarized parallel to the plane of incidence, so the Fresnel reflection coefficient is:

$$r = \frac{n_3 \cos \theta_1 - \left(1 - \left(\frac{\sin \theta_1}{n_3}\right)^2\right)^{\frac{1}{2}}}{n_3 \cos \theta_1 + \left(1 - \left(\frac{\sin \theta_1}{n_3}\right)^2\right)^{\frac{1}{2}}} \quad (21)$$

where $n_1 = 1$ and $\cos \theta_3$ has been rewritten using Snell's law. Total reflectance, R , is the square of the reflection coefficient or

$$R = |r|^2 \quad (22)$$

The quantities R and θ_1 are measured experimentally which leaves n_3 the only unknown in (21) and (22). A computer program was written to determine a value for n_3 given R and θ_1 . This value was then used in the computer program to determine values for n_2 and k_2 .

Interference Fringe Analysis

The three media model shown in Figure 4 is the one used for this analysis. The three assumptions stated in the introduction to this chapter apply. Added to these is the assumption that the index of refraction of medium three is less than that of medium two, which was true for all samples studied. Any incident light ray will be reflected and refracted at both interfaces, and the resultant light rays will trace the paths shown in Figure 4. The refracted rays at the second interface have been omitted because they do not enter into the analysis.

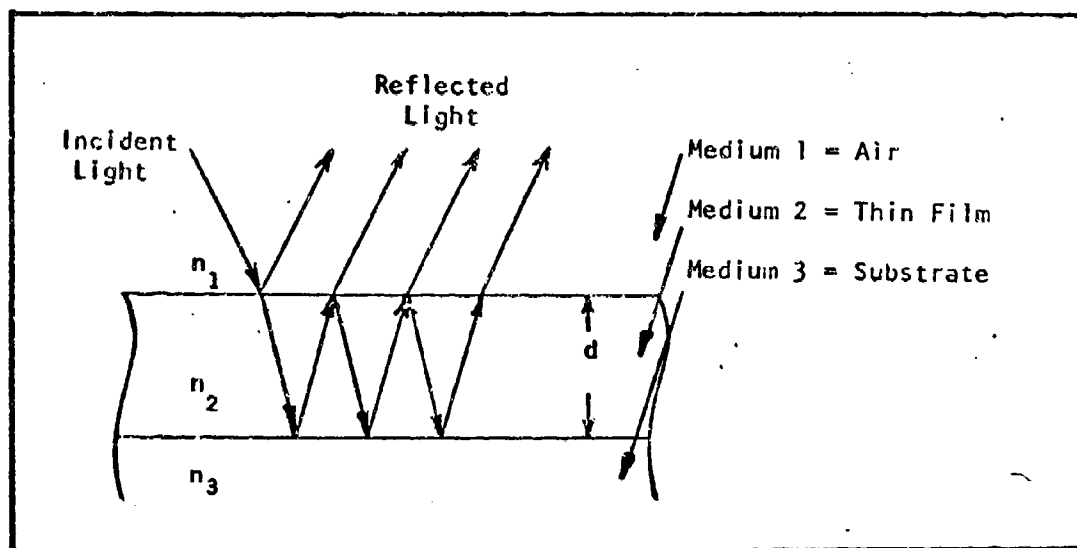


Fig. 4. Three Media Model Used in Interference Fringe Analysis

The reflected rays alternately interfere constructively and destructively as the wavelength of the incident light increases or decreases. A reflection spectrum then will have alternating reflectance maxima and minima as the wavelength increases or decreases. Although it is not obvious, the presence of an extinction coefficient in the thin film does not change the fringe spacing, as shown by computer calculations at Philips Laboratories (Ref 11:2346).

For a reflectance spectrum of a free standing film or of a film on a substrate where the index of refraction of the substrate is less than that of the film, the position of amplitude minima and maxima can be determined by the following relations (Ref 17:262-3).

$$2nd \cos \theta_2 = m/\nu \quad \text{MINIMA} \quad (23)$$

$$2nd \cos \theta_2 = (m + \frac{1}{2})/\nu \quad \text{MAXIMA} \quad (24)$$

where

- n = index of refraction of the film.
- d = physical thickness of the film.
- θ_2 = angle of refraction in the film.
- $\nu = \frac{1}{\lambda}$ = wavenumber of incident light.
- m = the order of the interference.

Using Snell's law, $\cos \theta_2$ can be rewritten in terms of θ_1 , the incident angle of the incident light.

$$\cos \theta_2 = \left(1 - \frac{\sin^2 \theta_1}{n^2} \right)^{\frac{1}{2}} \quad (25)$$

Now combining equation (25) with either equation (23) or equation (24)

one can obtain the same result for n .

$$n = \left[\frac{(\Delta m)^2}{4d^2 (\Delta v_{if})^2} + \sin^2 \theta_1 \right]^{\frac{1}{2}} \quad (26)$$

where

$\Delta m = m_i - m_f$ = number of fringes between the initial and final fringes counted.

$\Delta v_{if} = v_i - v_f$ = wavenumber difference between the initial and final fringe.

Equation (26) was then used to compute an index of refraction. The values for Δm and Δv were obtained from the reflection spectrum, and θ_1 and d were measured as outlined in Chapter III.

III. Experimental Samples, Equipment, Problems, Procedure, and Parameters

Introduction

This chapter is divided into five parts. The samples studied are discussed in the first part. The physical apparatus used to take measurements is discussed in the second part. The problems encountered during the course of the experiment and the experimental procedure used are presented in parts three and four, respectively. Finally, the reasons for choosing the final experimental parameters are presented in part five.

Samples

The coated samples were prepared, under government contract, by Optical Coating Laboratory, Inc. The materials under study were thermally vacuum evaporated onto polished potassium chloride blanks, $3/8$ inches thick and two inches in diameter. Two blanks were coated at the same time so there were normally two coatings of each thickness to test. Each side of each blank was half coated, and the coating on one side of a blank was rotated 90 degrees from the coating on the other side as shown in Figure 5.

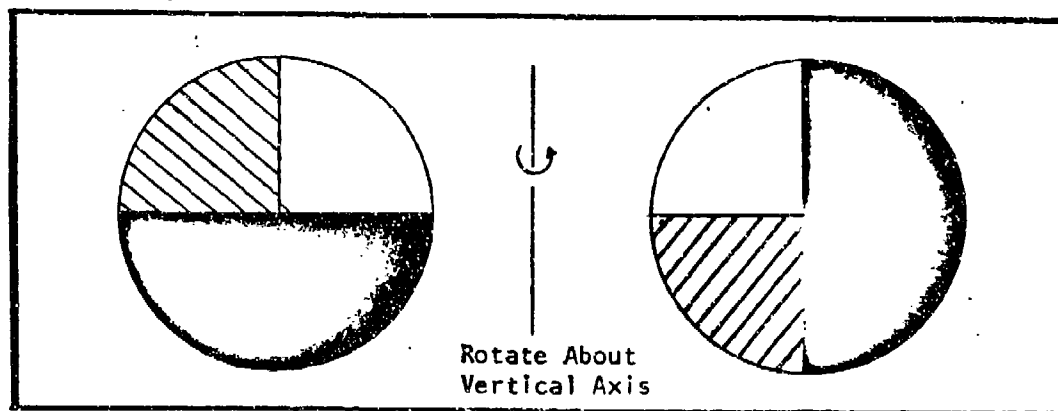


Fig. 5. View of Both Sides of a Coated Blank

Many of the coatings appeared much as a newly painted vertical wall does when the paint "runs". The details of the sample preparation were not available, so it is not known how this "running" could occur. The fact that these "runs" were actual discontinuities was confirmed by measurements with a Sloan M-100 angstrometer. In addition, almost all the coatings had apparent discontinuities and/or scratches. An individual description of each coating is presented in Appendix A. Although the samples were not physically good coatings, it was felt that a general idea of their optical constants might be obtained by analyzing their reflection spectra in accordance with the theory developed in Chapter II.

Apparatus

The reflection spectra of the seven thin film materials were recorded using a Perkin-Elmer 225 dual beam spectrophotometer with a reflectance attachment. The reflectance attachment was designed to be used for direct reflectance and consisted of two units. One unit was the mirror image of the other in order to match beam paths. These units were attached to one another by steel rods so that when the attachment was placed in the spectrophotometer sample compartment, one unit was in the sample beam path and the other unit was in the reference beam path. The placement of the attachment and the resulting beam paths are shown in Figure 6.

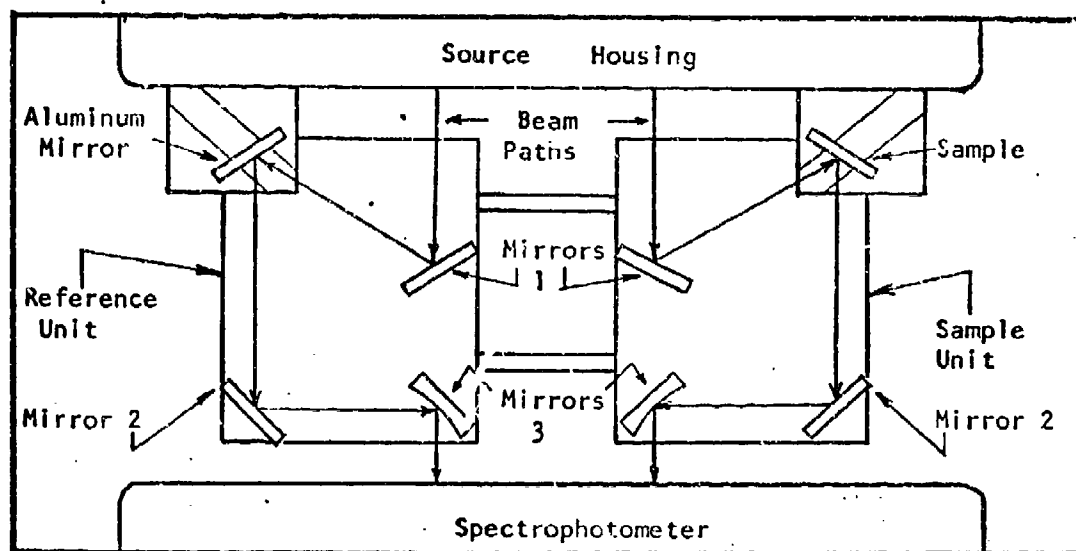


Fig. 6. Attachment Placement and Beam Paths

Figure 7 shows an expanded view of the unit that would be in the sample beam. Light from the source was reflected by mirror 1 onto the sample. The light was then reflected in turn to mirrors 2 and 3 and into the spectrophotometer. The reference beam unit had an aluminum reference mirror in the sample position.

The incident angle of the light onto the sample was variable from about 22 to 70 degrees. This was possible because mirror 1 could be placed in one of three positions, and the sample mount was on a slide which had a travel of about three centimeters, as shown in Figure 7. All mirrors and the sample could be rotated about their vertical axes.

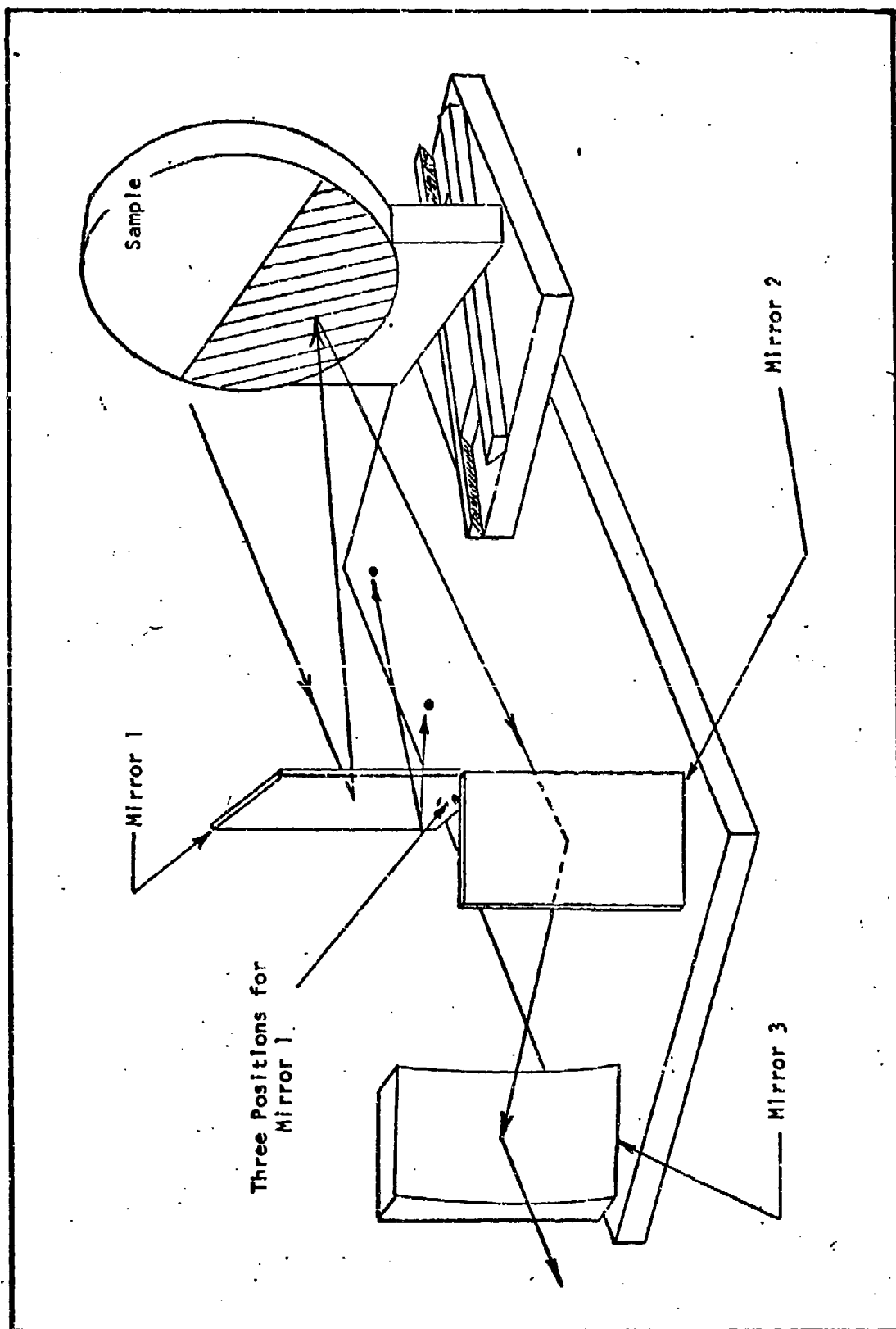


Fig. 7. Sample Unit

Theoretically, any incident angle could be chosen between 22 and 70 degrees. However, it was difficult to align the attachment to a specific incident angle, because it was a trial and error process. One normally positioned mirror 1 where he thought it should be. Then the sample and remaining mirrors were aligned with respect to mirror 1. If the resulting angle was not correct the process was started over again.

The incident angle was measured indirectly. The angle that the central ray of the source beam made with the axes of the source housing was known. Additionally, the sides of the attachment were approximately perpendicular and parallel to the axes of the source housing (within two degrees). So small protractors were placed under mirror 1 and the sample mount. These protractors measured the angles that the mirror and sample made with the sides of the attachment. Since the angles that the incident beam, mirror, and sample made with respect to a common reference were known, the incident angle could be determined by geometry.

The light was polarized parallel to the plane of incidence with a number 186-0240, Perkin-Elmer wire grid polarizer. This polarizer had a spectral range of 2.5 to 35 microns. It was placed in front of the entrance slit of the spectrophotometer, since this was a common point of the sample and reference beams.

Since only half the substrate was coated as described previously, the top part of the incident light beam had to be masked to insure that only the coated half of the sample was illuminated. This was done two ways. First a jig was built to mask the beam just before it reached the sample and aluminum reference mirror. Second, a mask was built to

fit directly over mirror 1. The second procedure proved to be the more convenient because this mask did not require realignment with every sample change. In either case, the sample and reference beam were masked the same amount. It was found that the best reflection spectra were obtained when as large an area of the coating as possible was illuminated.

Experimental Problems

Optical Alignment. Optical alignment of the system was the biggest problem. This occurred both in the vertical and horizontal planes. To align the system in the horizontal plane the spectrophotometer housing was opened and the light beams followed through the system. The attachment mirrors were rotated until the spectrophotometer entrance slit was illuminated by both the reference and sample beams. Then the housing was closed and the fine alignment accomplished by slowly rotating mirror 3 on both units. First, mirror 3 on the reference unit was slowly rotated until the scale reading was lowest. Then mirror 3 of the sample unit was slowly rotated until the scale reading was highest. This part of the alignment procedure was critical as a 2-3 degree rotation would result in a scale deflection of five to ten percent or more.

The vertical alignment problem became evident whenever a filter was moved in front of the entrance slit to the spectrophotometer. The filter was placed in the beam at certain wavelengths to protect the spectrophotometer detector. If both beams did not strike the filter at the same angle, then one beam was scattered differently than the other. Thus, more energy of one beam would enter the spectrophotometer

and cause a scale deflection of 5 to 20 percent. This deflection could theoretically be reduced to zero by proper alignment of the attachment mirrors. Practically this was impossible because there were eight reflecting surfaces to adjust. The deflection was significantly reduced by carefully tilting mirror 3 on each unit so that the sample and reference beams illuminated the spectrophotometer entrance slit equally. Then mirror 2 of one unit was tilted in small increments. After each increment the spectrophotometer was run through the portions of the spectrum where the filter came into the beams to see if the deflection was within acceptable limits. This procedure was continued until the deflection was within acceptable limits; normally about plus five percent.

Light Spillover. The light beam from the source housing was a converging beam. Since all the reflecting surfaces were flat, except mirror 3, the reflected beam would at times "spill" around the edges of one of the mirrors. To minimize the effect of this, the spillover was matched as much as possible on both units of the attachment.

Sample and Reference Mirror Mounts. The reflectance attachment mounts for the sample and reference mirror did not provide a secure mount. So new mounts were made out of balsa wood. Balsa wood was used because it was easy to work with and any mount could normally be made in a day. The balsa wood mounts were constructed to slip over the attachment mounts. The balsa wood mounts proved very durable and were more than adequate for the experiment.

Experimental Procedure

At the beginning of each day, two 100% reflection spectra were recorded with an aluminum mirror in the reference unit and a United States Bureau of Standards gold standard mirror in the sample unit. Two 100% spectra were run to check the spectrophotometer reproducibility and to get an average 100% reflection spectrum. Then without changing any controls or mirror positions the gold standard mirror was replaced with coated samples and the reflection spectra of the coatings were recorded. There normally were two coatings of the same thickness for each substance so the two spectra for that thickness were averaged. After all the spectra were recorded the reflectance values were normalized at every half micron as shown in Appendix B. This normalization process was required because the 100% spectra could not be recorded at full scale deflection (100%). They were normally recorded at about 90% scale deflection. This was due to the recording pen deflection caused by vertical mirror misalignment discussed in the experimental problems section of this chapter. The wavenumber positions where the reflectance maxima and minima occurred were recorded for each spectrum, and then averaged for coatings of the same thickness. This information is presented in Appendix C. This information was then used to compute an index of refraction for each material using equation (26). The computed indices are presented in Appendix D.

The physical thicknesses of the samples were measured using a Sloan M-100 angstrometer. This angstrometer works on the principle of Fizeau fringes with a sodium source. This procedure would often result in a small cut in the thin film coatings, so this measurement was left

until all reflection spectra had been recorded. Also, only one coating of each thickness was measured so as to keep from damaging any more samples than necessary. The validity of this procedure was checked by measuring two coatings that were supposed to be the same thickness for two different materials. In both materials the measurement of the two coatings was the same.

Parameters

The parameters chosen for this experiment, such as incident angle, plane of polarization, etc., were dictated by the use of the total reflectance analysis discussed in Chapter II. The reason for choosing light polarized parallel to the incident plane was that parallel polarized light is more sensitive to changes in the index of refraction, n_2 , and the extinction coefficient, k_2 , and is more tolerant of measurement error than perpendicular polarized light (Ref 16:1200, 1202).

Three angles of incidence were used because any ambiguities caused by multiple intersections of two n_2 - k_2 plots would be resolved by a third n_2 - k_2 plot (Ref 16:1201). The values of the incident angles used in this experiment were chosen because the highest crossing angle between two n_2 - k_2 plots occurs when one plot is the result of measurements taken at near normal incidence and the other plot is the result of measurements taken at the principle angle of incidence. The principle angle of incidence is the angle where the phase difference between the reflectance of parallel polarized light and perpendicular polarized light is 90 degrees (Ref 16:1200). This angle is very close to the Brewster angle, so the 51 and 63 degree angles were chosen on this basis. The 22 degree angle was as close to normal incidence as the attachment would

go.

The fact that three incident angles were used also gave a cross-check on the computation of the index of refraction using equation (26). Since the interference fringes occurred at about the same place for all incident angles, any discrepancies between spectra would be immediately detectable by how well the calculated indices agreed.

IV. Results and Conclusions

Introduction

This chapter is divided into four parts. The results of the experimental spectra are dealt with in section one. The results of the total reflectance analysis and the interference fringe analysis are discussed in sections two and three, respectively. Finally, the indices of refraction of the thin film coatings are compared with the indices of refraction of the bulk materials in section four. Conclusions are broken down in the same manner and presented in their respective sections.

It should be pointed out that the numerical results may or may not be correct because the equations used to determine numerical results are based on an idealized three media model, and all but one thin film coating displayed visible inhomogeneities. However, the numerical results probably give fairly accurate indications of any trends.

Experimental Spectra

The experimental spectra were very consistent. Each thin film spectrum displayed the interference fringes discussed in Chapter II. Additionally, for each sample, the maximum amplitude of the spectra decreased as the incident angle increased. This is to be expected because the incident light was polarized parallel to the incident plane, and the Brewster angles of these materials lie between 65 and 75 degrees. The wavelength distance between fringes increased as wavelength increased, which is to be expected for a material with a fairly constant index of refraction throughout the spectrum. The wavenumber,

$\frac{1}{\lambda}$, distance between fringes, however, gradually decreased as the wavelength increased. This indicates that the indices of refraction of these materials increase as wavelength increases. Figures 8, 9, and 10 are reduced images of actual raw data and very graphically show the interference fringes mentioned before. The spectra are cadmium selenide, thickness 2.59 microns, at incident angles of 22, 51, and 63 degrees, respectively.

Another phenomena that can be seen in Figures 9 and 10 is a hump in the spectrum that occurs from 13.5 to about 16.0 microns. This hump was present on numerous spectra at the 51 and 63 degree incident angles. Every time it occurred, the hump rose sharply at 13.5 microns, peaked at 14.0 microns, and fell off to what appeared to be a normal curve at 15.5 to 16.0 microns. This hump in the spectra is probably an idiosyncrasy of the spectrophotometer, because it occurred in such a consistent manner. However, the cause of this hump should be investigated further, because, if the hump is actually there, it indicates a sharp rise in the index of refraction. The best way to check this would be to record the spectra for the same materials on a different spectrophotometer.

The raw data in Figures 8, 9, and 10 also show that the spectra are recorded out to 22.2 microns. All spectra were recorded this far out in the Infrared, however, the 100% spectra became erratic after 17.0 microns. Therefore, no values were normalized after 17.0 microns, and the position of fringe maxima after 17.0 microns may or may not be correct.

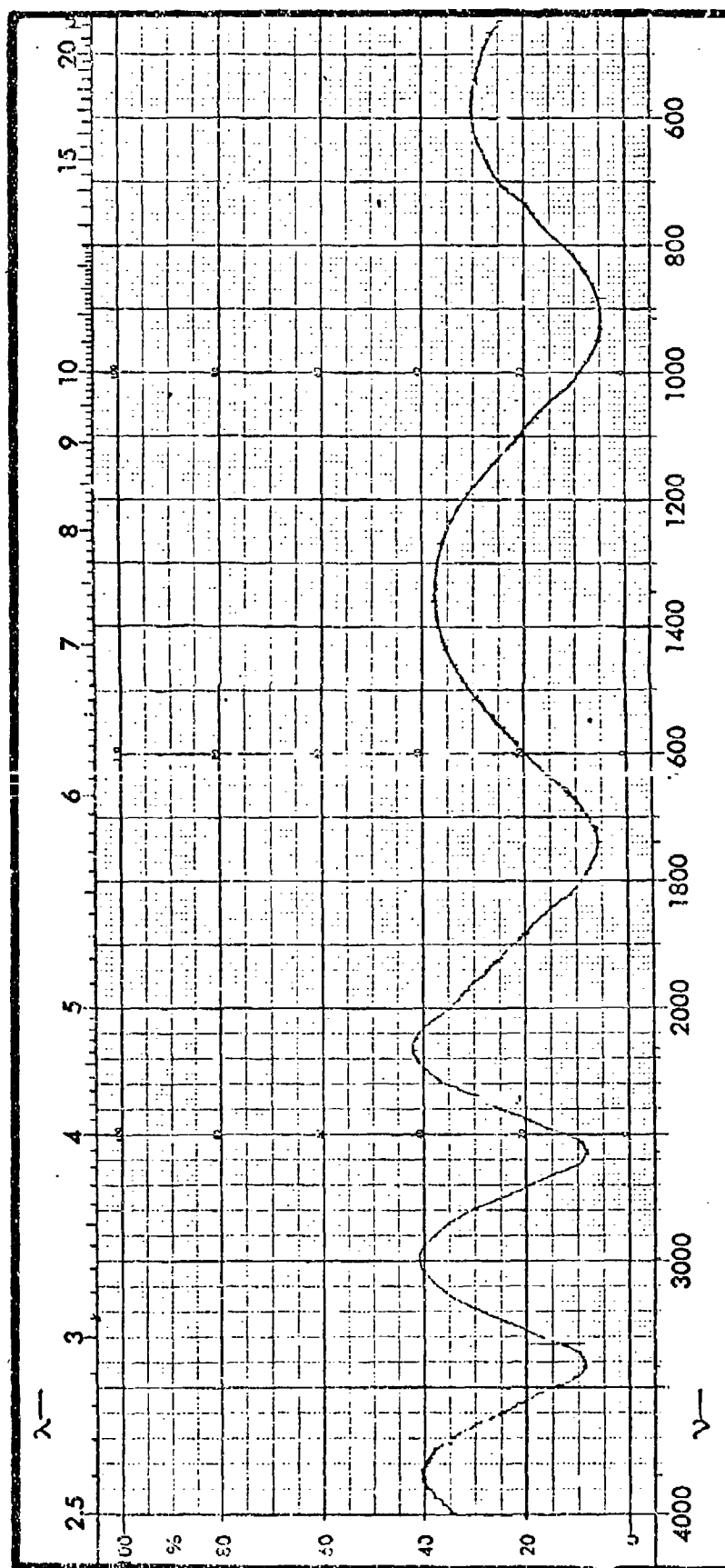


Fig. 8. Reflection Spectrum for 22° Incident Angle

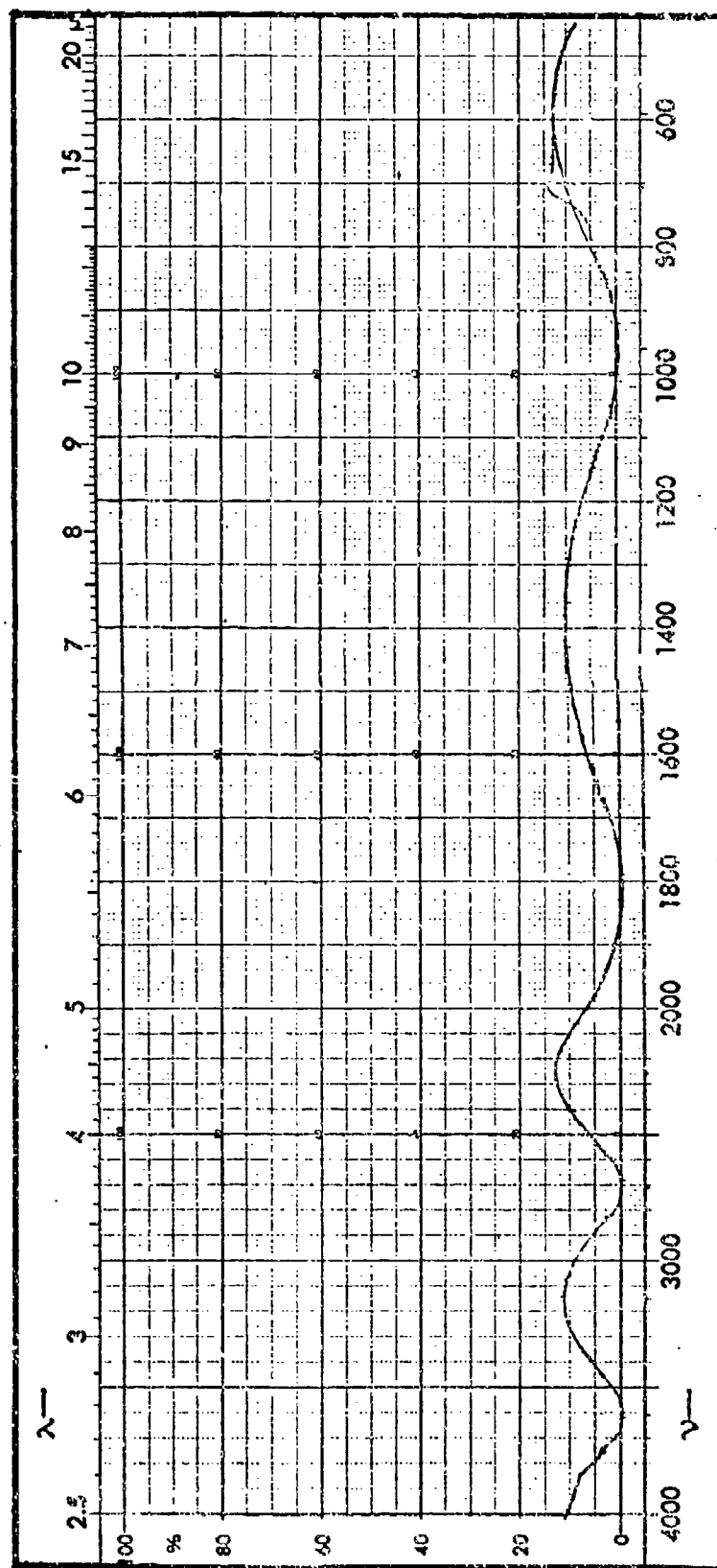


Fig. 9. Reflection Spectrum for 51° Incident Angle

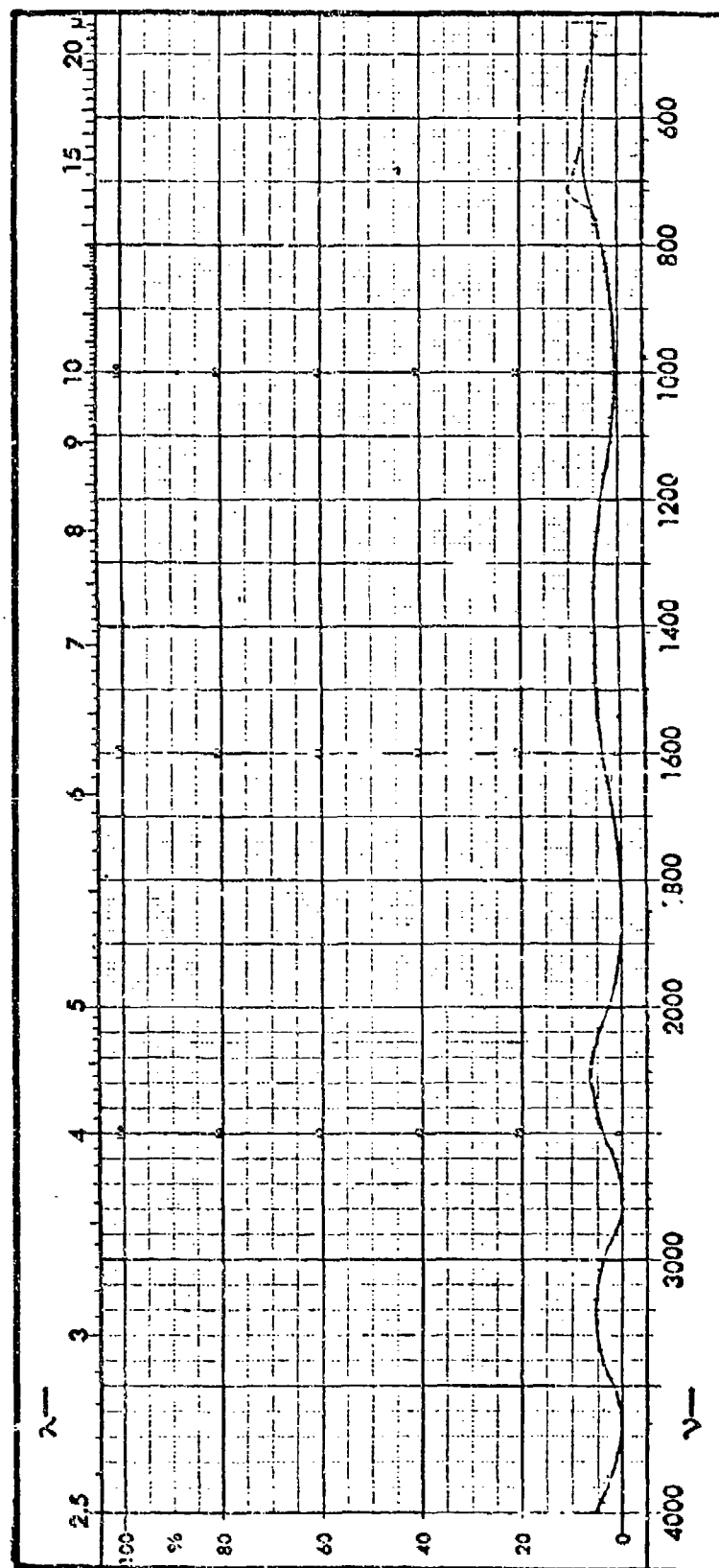


Fig. 10. Reflection Spectrum for 63° Incident Angle

The erratic behavior after 17.0 microns is caused by the reflectance attachment, because the spectrophotometer records a straight 100% spectrum out to 35.0 microns without any attachment. This behavior could probably be eliminated by a more exacting optical alignment of the mirrors on the attachment and by using curved mirrors to image the source onto the sample. Larger mirrors should also be used to eliminate the spillover described in Chapter II. This would help because there were detectable inhomogeneities in both the sample and reference beams.

Total Reflectance Analysis

This portion of the analysis was disappointing, as matching k values for all given n values could not be determined by computer calculations as described in Chapter II. The computer program was first set up to search for k values from zero to one. Only 25% of the matching k values could be found, and all were less than one. The program was then set up to search for k values from zero to ten. This time 35% of the matching k values were found. Again, all were less than one. However, where a k value was found by both programs for the same n value, the two k values were different in all cases. This indicates that the theory is insensitive to changes in k values. According to Harrick, reflected light is relatively insensitive to the extinction coefficient (Ref 11: 2346).

A significant point is that whenever the programs were unable to find matching k values, the theoretical reflectance was always greater than the measured reflectance. This indicates that the inhomogeneities in the thin films cause a reduction in reflectance from the idealized

case assumed for the theory. This reduction is probably due to light being scattered by the inhomogeneities. Another possibility is that the normalized experimental reflectance values used in the computer program were incorrect. This could be due to an error in the reflectance of the gold standard mirror, or an error in the measured experimental reflectance, or both.

An error in the normalized data in Appendix B could be introduced because the gold standard mirror was calibrated at a 9 degree incident angle, and the raw data was generated at higher incident angles. The calibrated values of reflectance for the gold standard mirror varied from 0.985 at 2.5 microns to 0.987 at 17.0 microns. Since the incident light was polarized parallel to the incident plane, the reflectance of the gold standard could change if it had an effective Brewster angle. A search of the literature showed that an evaporated gold mirror displays no such change in reflectance in the infrared for a 23 degree incident angle (Ref 5:264). Other sources list values of refractive index for evaporated gold mirrors that imply that any effective Brewster angle is about 40 to 50 degrees for 2.5 microns, 60-70 degrees for 3.0 microns, and greater than 70 degrees for longer wavelengths (Ref 19, 20). These Brewster angles were calculated using the relation $\cot \theta_B = \frac{l}{n}$, where n = refractive index of gold, l = refractive index of air, and θ_B = Brewster angle. If there were an effective Brewster angle though, the 100% spectra recorded at the beginning of each day should go to zero reflectance at 2.5 or 3.0 microns. No such phenomenon occurred.

The literature values apply to evaporated gold mirrors, which had different thicknesses and were prepared under different conditions than

the gold standard used. So in order to really verify the normalized values one needs to calibrate the gold standard mirror at angles and wavelengths of interest. This could possibly be done with the Perkin-Elmer 225 Spectrophotometer working in a single beam mode with an electrical test signal (Ref 3:23).

The experimental reflectance measurements were also probably in error although it really cannot be determined by how much. The magnitude of this error could be reduced if the vertical scale of the spectrophotometer could be expanded. This could be done with an attenuator in the spectrophotometer reference beam. However, one would need to know the absolute reflectance or transmittance of a sample in the sample beam in order to do an accurate expansion. Although a difficult problem, this possibility should be investigated, because of the possibility of obtaining greater accuracy.

Finally, the computer program should be tested with theoretical data to see if it does give correct answers. This is the next logical step, since the programs do not yield answers for the experimental data. This was not done due to insufficient time.

Interference Fringe Analysis

The indices of refraction for each material are presented in Appendix D. This section will be a general synopsis of these results. The results generally show four phenomena: (1) the refractive index increases with wavelength, (2) the refractive index rises sharply around 10.0 microns, (3) three of the thin film materials displayed an index change with a thickness change, and (4) the minimum to

minimum fringes yielded more consistent results than maximum to maximum fringes.

The refractive index for all thin film materials, except germanium, increased as the wavelength increased. In some materials this increase was about 0.1, while in many others it was about 0.5. The analysis for germanium did not have consistent results. Using the maximum to maximum interference fringes, the refractive index of germanium increased, while using the minimum to minimum interference fringes the refractive index decreased slightly.

The refractive index of all materials rose sharply at about 10.0 microns. Up to about 10.0 microns most materials showed a modest increase in the value of the refractive index. The interference fringe that fell on either side of 10.0 microns was always a maximum to maximum fringe. Since the spectrophotometer gave erratic results after 17.0 microns, the position of any interference fringe maximum after about 15.0 microns may not be the wavelength at which the true interference maximum occurs. In order to verify this, some spectra should be spot checked after the reflectance attachment is fitted with new mirrors and realigned.

Three of the thin film materials showed a marked change in the refractive index with a change in film thickness. The refractive indices for zinc sulfide, cadmium selenide, and germanium changed on the order of 0.2 for film thickness changes of 0.06, 0.18, and 0.06 microns respectively. This indicates that the refractive index may be thickness dependent, and the phenomena should be investigated further. Probably the best way to check this would be to take measurements on a

large number of samples of different thicknesses.

For most analyses the minimum to minimum fringes gave more moderate changes in the refractive indices than the maximum to maximum fringes. The refractive index always increased faster using the maximum to maximum fringes. This indicates that the fringe maxima are skewing toward shorter wavelengths as wavelength increases, while fringe minima are remaining relatively stationary. This is portrayed in Figure 11, which is a schematic of fringe maxima and minima for cadmium selenide, thickness 2.59 microns. Since in equation (26) $n \propto \frac{1}{(\Delta v)^2}$, it can be seen that the fringe maxima skewing to the left result in a more rapid increase for n than the fringe minima do.

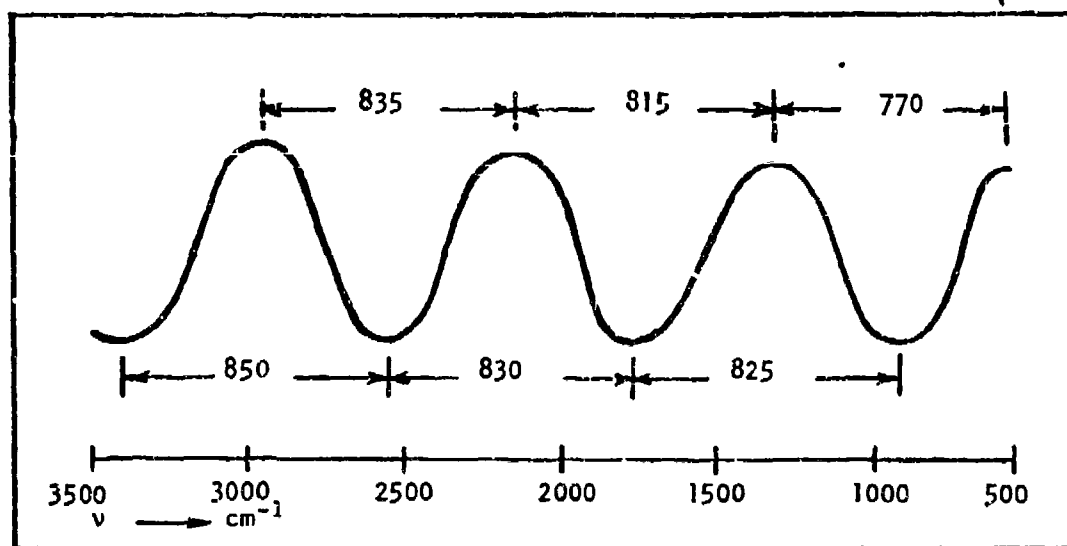


Fig. 11. Wavenumber Difference Between Fringes for CdSe
for 22° Incident Angle

More spectra would help to determine the cause of this. It would also be a great aid to be able to get interference fringes further out in the infrared to find out if this phenomena continues. Since this more

rapid increase of n for fringe maxima occurs for all samples tested, the phenomena may be due to characteristics of the reflectance attachment used in the spectrophotometer. The best way to check this would be to record reflection spectra on the same samples using a different or improved reflectance attachment.

Bulk vs Thin Film Index

This section will deal with the comparison of the computed indices of refraction with bulk material indices reported in the literature. The thin film indices used for the comparison will be the ones computed from minimum to minimum fringes because these were more consistent than the indices computed from maximum to maximum fringes. The comparison will be for the 10.0 micron region since this is the proposed wavelength region of use for these materials.

Material	Bulk Index	Thin Film Index
ZnS	2.20	2.16/2.30
ZnSe	2.41	2.53/2.58
Ge	4.00	4.03/4.19
CdS	2.25	2.88/2.93
CdTe	2.67	2.71/2.74
ZnTe	3.00*	2.92/2.97
CdSe	2.4	2.38/2.55

Fig. 12. Indices of Refraction in 10.0 μ Region

*Reported Thin Film Index

Figure 12 lists both bulk and thin film indices. The first five bulk indices are reported by Eastman Kodak Company (Ref 6:13, 14). The index listed for ZnTe is actually an index for a ZnTe thin film on a ZnSe substrate. This figure was reported by Hughes Research Laboratories at the October 1973 Conference

on High Power Infrared Laser Window Materials. The bulk index for CdSe

was reported by Optical Coating Laboratory, Inc., in a letter accompanying the sample shipment. It is not known how the bulk indices were determined.

For most materials the thin film indices agree favorably with the reported bulk values. However, the thin film index for CdS is significantly higher than the bulk value. The reason for this large difference is not known and should be investigated further. From Figure 12, it appears that generally the thin film refractive index is approximately the same as the bulk material's refractive index. However, this approximation may or may not be valid enough to design AR coatings. To be accurate, the index of any thin film material under consideration, needs to be measured with the thin film coating on the same substrate with which the coating is to be used.

V. Recommendations

The primary recommendation is to improve the reflectance attachment. This can be done by replacing both mirrors 1 and 2 on both units of the reflectance attachment. They should be replaced with curved mirrors to focus the incident light beam onto the sample and mirror 3, respectively. These mirrors should be large enough to prevent light spillover. The first mirrors on each unit should also be placed in the center of the incident beam. They are presently about 2.0mm away from the center of that beam.

The next recommendation is to obtain better quality coatings and conduct the same or similar tests with them. How much effect the poor quality of the tested coatings had on the results is not known. Results from good quality coatings would be of great benefit in determining the validity of results presented in this thesis.

The final recommendation is to coat a substrate blank completely. This would give more area for the incident beam to illuminate. Also, the blank should be coated on only one side and the other side frosted, so that there will be no contribution to total reflectance from the back surface.

Bibliography

1. Armaly, B. F., et al. "Restrictions on the Inversion of the Fresnel Reflectance Equations". Applied Optics, 11:2907-2910 (December 1972).
2. Bennett, J. M. and M. J. Booty. "Computational Method for Determining n and k for a Thin Film from the Measured Reflectance, Transmittance, and Film Thickness". Applied Optics, 5:41-43 (January 1966).
3. Bodenseewerk, Perkin; Elmer and Co. Model 225 Infrared Grating Spectrophotometer, Description and Instructions.
4. Born, M. and E. Wolf. Principles of Optics. London: Pergamon Press, 1959.
5. DeWitt, D. P. and Y. S. Touloukian. Thermal Radiative Properties, Metallic Elements and Alloys. New York: IFI/Plenum, 1970.
6. Eastman Kodak Company. Kodak Intran Infrared Optical Materials. Kodak Publication U-72, 1971.
7. Goell, J. E. and R. D. Standly. "Effect of Refractive Index Gradients on Index Measurement by the Abeles Method." Applied Optics, 11:2502-2505 (November 1972).
8. Gottlieb, M. "Optical Properties of Lithium Fluoride in the Infrared". Journal of the Optical Society of America, 50: 343-349 (April 1960).
9. Hadley, L. N. and D. M. Dennison. "Reflection and Transmission Interference Filters". Journal of the Optical Society of America, 37:451-456 (June 1947).
10. Hanson, W. N. "Optical Characterization of Thin Films: Theory". Journal of the Optical Society of America, 63:793-802 (July 1973).
11. Harrick, N. J. "Determination of Refractive Index and Film Thickness from Interference Fringes". Applied Optics, 10:2344-2349 (October 1971).
12. Hass, G. and R. E. Thun. Physics of Thin Films, Volume II. New York: Academic Press, 1964.
13. ----- Physics of Thin Films, Volume IV. New York: Academic Press, 1967.
14. Heitman, W. "Reactively Evaporated Films of Scandia and Yttria". Applied Optics, 12:394-397 (February 1973).

15. -----, "Vacuum Evaporated Films of Aluminum Fluoride". Thin Solid Films, 5:61-67 (1970).
16. Hunter, W. R. "Errors in Using the Reflectance vs Angle of Incidence for Measuring Optical Constants". Journal of the Optical Society of America, 55:1197-1204 (October 1965).
17. Jenkins, F. A. and H. E. White. Fundamentals of Optics. New York: McGraw-Hill Book Co., 1957.
18. Juenker, D. W. "Digital Evaluation of the Complex Index of Refraction from Reflectance Data". Journal of the Optical Society of America, 55:295-299 (March 1965).
19. Lenham, A. P. and D. M. Treherne. "Applicability of the Anomalous Skin Effect Theory to the Optical Constants of Cu, Ag, and Au in the Infrared". Journal of the Optical Society of America, 56:683-685 (May 1966).
20. Motulevich, G. P. and A. A. Shubin. "Influence of Fermi Surface Shape in Gold in the Optical Constants". Soviet Physics, JETP, 20:560-564 (March 1965).
21. Morrissey, B. W. and C. J. Powell. "Interpolation of Refractive Index Data". Applied Optics, 12:1588-1591 (July 1973).
22. Nestell, J. E. and R. W. Christy. "Derivation of Optical Constants of Metals from Thin Film Measurements at Oblique Incidence". Applied Optics, 11:643-651 (March 1972).
23. -----, "Optics of Thin Metal Films". American Journal of Physics, 39:313-320 (March 1971).
24. Ruiz-Urbieto, M. "Film Thickness and Refractive Indices of Dielectric Films on Dielectric Substrates". Journal of the Optical Society of America, 61:1392-1396 (October 1971).
25. Ruiz-Urbieto, M. and E. M. Sparrow. "Refractive Index, Thickness and Extinction Coefficient of Slightly Absorbing Thin Films". Journal of the Optical Society of America, 62:931-937 (August 1972).
26. Ruiz-Urbieto, M., et al. "Methods for Determining Film Thickness and Optical Constants of Films and Substrates". Journal of the Optical Society of America, 61:351-359 (March 1971).
27. Stone, J. M. Radiation and Optics. New York: McGraw-Hill Book Co., 1963.
28. Stratton, J. A. Electromagnetic Theory. New York: McGraw-Hill Book Co., Inc., 1941.

29. Tousey, R. "On Calculating the Optical Constants from Reflection Coefficients". Journal of the Optical Society of America, 29: 235-239 (June 1939).
30. Whang, U. S., et al., "Slope Method for Determining Extinction Coefficients". Journal of the Optical Society of America, 63: 305-308 (March 1973).
31. Zwerdling, S. "Evaluation of Refractive Index from Interference-Fringe Transmission Spectra". Journal of the Optical Society of America, 60:787-790 (June 1970).

Appendix A
Condition of Coatings

<u>Coating Material</u>	<u>Measured Thickness</u>	<u>Brief Description of Coating</u>
Zinc Sulfide	2.71 microns	Large scratch through center, unuseable.
Zinc Sulfide	2.71 microns	Mottled, very finely scratched.
Zinc Sulfide	2.65 microns	Good coating.
Zinc Sulfide	2.65 microns	Mottled, very finely scratched.
Germanium	1.27 microns	Mottled, very finely scratched.
Germanium	1.27 microns	Very finely scratched.
Germanium	1.33 microns	Mottled, very finely scratched.
Germanium	1.33 microns	Very finely scratched.
Cadmium Selenide	2.41 microns	Coating ran, numerous pinholes in coating.
Cadmium Selenide	2.41 microns	Extensively scratched, unuseable.
Cadmium Selenide	2.59 microns	Coating ran, numerous pinholes in coating.
Cadmium Selenide	2.59 microns	Intermittent scratches, a few pinholes in coating.
Cadmium Telluride	2.06 microns	Coating ran.
Cadmium Telluride	2.06 microns	Coating ran.
Cadmium Telluride	2.09 microns	Coating ran.
Cadmium Telluride	2.09 microns	Coating ran, slightly fogged.

<u>Coating Material</u>	<u>Measured Thickness</u>	<u>Brief Description of Coating</u>
Zinc Selenide	2.06 microns	Slightly fogged.
Zinc Selenide	2.06 microns	Slightly fogged.
Zinc Selenide	2.03 microns	Slightly fogged.
Zinc Selenide	2.03 microns	Slightly fogged.
Zinc Telluride	1.71 microns	Coating ran, slightly fogged.
Zinc Telluride	1.71 microns	Coating ran, very finely scratched.
Zinc Telluride	1.74 microns	Coating ran, slightly fogged.
Zinc Telluride	1.74 microns	Coating ran, very finely scratched.
Cadmium Sulfide	1.80 microns	Very finely scratched.
Cadmium Sulfide	1.80 microns	Very finely scratched.
Cadmium Sulfide	1.83 microns	Very finely scratched.
Cadmium Sulfide	1.83 microns	Very finely scratched.

Appendix B

Tables of Normalized Experimental Reflectances

The following tables contain the normalized experimental reflectances of the seven film materials plus the bare substrate. The tables are arranged so that the reflectances are given at every half micron for each incident angle. The reflectance at 10.6 microns is given instead of 10.5 microns, because 10.6 microns is the wavelength of the CO_2 laser.

The reflectance values were normalized in the following manner. At the beginning of each day, two 100% reflectance spectra were recorded with an aluminum mirror in the reference beam and a United States Bureau of Standards gold standard mirror in the sample beam. The values from the two 100% spectra were averaged. Then without any control changes the reflectance spectra of the coatings were recorded. There normally were two coatings of the same thickness for each substance so the two spectra for that thickness were averaged.

Now at a particular wavelength let the following symbols be defined:

- R_a = absolute reflectance of the aluminum mirror placed in the reference beam.
- R_g = absolute reflectance of the gold standard mirror placed in the sample beam.
- R_s = absolute reflectance of the coating on a substrate placed in the sample beam.
- M_a = averaged measurement taken from the 100% spectrum.
- M_s = averaged measurement taken from the sample spectrum.

Then the value from the 100% spectrum is

$$M_g = \frac{R_g}{R_a} \quad (3)$$

and the value from the sample spectrum is

$$M_s = \frac{R_s}{R_a} \quad (4)$$

Now if the same aluminum mirror is used in the reference beam for both the 100% and sample spectra, then R_a is the same in either case. So equating R_a and rearranging the results, one gets

$$R_s = \frac{M_s}{M_g} R_g \quad (5)$$

Since the Bureau of Standards had already calibrated the reflectance of the gold standard, the only unknown is R_s which is the normalized value desired.

Table I

Table of Normalized Experimental Reflectances for Zinc Sulfide
Film Thickness: 2.71 Microns

Wavelength/Wavenumber (microns) (cm ⁻¹)		Incident Angle		
		22 Degrees	51 Degrees	63 Degrees
2.5	4000	0.310	0.054	0.005
3.0	3333	0.302	0.093	0.345
3.5	2857	0.242	0.002	0.000
4.0	2500	0.157	0.082	0.032
4.5	2222	0.354	0.088	0.002
5.0	2000	0.268	0.019	0.006
5.5	1818	0.095	0.006	0.022
6.0	1667	0.122	0.057	0.024
6.5	1538	0.263	0.094	0.039
7.0	1428	0.347	0.103	0.039
7.5	1333	0.366	0.094	0.031
8.0	1250	0.351	0.069	0.021
8.5	1176	0.306	0.050	0.012
9.0	1111	0.234	0.022	0.006
9.5	1053	0.186	0.008	0.006
10.0	1000	0.118	0.000	0.004
10.6	943	0.081	0.000	0.006
11.0	909	0.074	0.000	0.006
11.5	870	0.085	0.012	0.008
12.0	833	0.107	0.017	0.010
12.5	800	0.155	0.037	0.012
13.0	769	0.185	0.052	0.014
13.5	741	0.207	0.063	0.018
14.0	714	0.239	0.075	0.021
14.5	690	0.260	0.080	0.024
15.0	667	0.271	0.082	0.021
15.5	645	0.276	0.082	0.020
16.0	625	0.277	0.082	0.020
16.5	606	0.276	0.077	0.022
17.0	588	0.271	0.076	0.018

Table II

Table of Normalized Experimental Reflectances for Zinc Sulfide
Film Thickness: 2.65 Microns

Wavelength/Wavenumber (microns) (cm ⁻¹)		Incident Angle		
		22 Degrees	51 Degrees	63 Degrees
2.5	4000	0.268	0.090	0.036
3.0	3333	0.137	0.057	0.022
3.5	2857	0.301	0.040	0.007
4.0	2500	0.111	0.036	0.014
4.5	2222	0.342	0.096	0.034
5.0	2000	0.310	0.052	0.012
5.5	1818	0.116	0.000	0.001
6.0	1667	0.099	0.021	0.013
6.5	1538	0.235	0.069	0.027
7.0	1428	0.329	0.094	0.034
7.5	1333	0.366	0.095	0.032
8.0	1250	0.358	0.087	0.024
8.5	1176	0.319	0.064	0.015
9.0	1111	0.259	0.040	0.010
9.5	1053	0.200	0.017	0.006
10.0	1000	0.143	0.003	0.002
10.6	943	0.090	0.000	0.001
11.0	909	0.074	0.000	0.002
11.5	870	0.083	0.002	0.006
12.0	833	0.101	0.009	0.010
12.5	800	0.137	0.020	0.011
13.0	769	0.175	0.032	0.015
13.5	741	0.197	0.049	0.018
14.0	714	0.220	0.063	0.020
14.5	690	0.250	0.071	0.021
15.0	667	0.267	0.078	0.021
15.5	645	0.269	0.080	0.020
16.0	625	0.273	0.080	0.022
16.5	606	0.270	0.076	0.019
17.0	588	0.266	0.076	0.018

Table III

Table of Normalized Experimental Reflectances for Germanium
Film Thickness: 1.27 Microns

Wavelength/Wavenumber (microns) (cm ⁻¹)		Incident Angle		
		22 Degrees	51 Degrees	63 Degrees
2.5	4000	0.617	0.232	0.170
3.0	3333	0.732	0.401	0.325
3.5	2857	0.141	0.000	0.002
4.0	2500	0.684	0.388	0.317
4.5	2222	0.724	0.347	0.271
5.0	2000	0.359	0.063	0.039
5.5	1818	0.224	0.103	0.094
6.0	1667	0.606	0.310	0.257
6.5	1538	0.735	0.407	0.337
7.0	1428	0.770	0.427	0.354
7.5	1333	0.744	0.398	0.323
8.0	1250	0.689	0.338	0.265
8.5	1176	0.694	0.255	0.204
9.0	1111	0.439	0.158	0.108
9.5	1053	0.291	0.070	0.053
10.0	1000	0.151	0.013	0.010
10.6	943	0.093	0.006	0.009
11.0	909	0.148	0.046	0.040
11.5	870	0.250	0.101	0.076
12.0	833	0.360	0.165	0.118
12.5	800	0.457	0.210	0.166
13.0	769	0.534	0.249	0.201
13.5	741	0.588	0.289	0.234
14.0	714	0.635	0.323	0.260
14.5	690	0.663	0.349	0.280
15.0	667	0.685	0.368	0.298
15.5	645	0.697	0.380	0.309
16.0	625	0.701	0.390	0.321
16.5	606	0.702	0.396	0.323
17.0	588	0.695	0.396	0.327

Table IV

Table of Normalized Experimental Reflectances for Germanium
Film Thickness: 1.33 Microns

Wavelength/Wavenumber (microns) (cm ⁻¹)		Incident Angle		
		22 Degrees	51 Degrees	63 Degrees
2.5	4000	0.613	0.265	0.182
3.0	3333	0.684	0.395	0.321
3.5	2857	0.146	0.003	0.001
4.0	2500	0.644	0.382	0.314
4.5	2222	0.688	0.355	0.279
5.0	2000	0.362	0.072	0.048
5.5	1818	0.196	0.094	0.089
6.0	1667	0.559	0.304	0.250
6.5	1538	0.687	0.404	0.333
7.0	1428	0.727	0.427	0.350
7.5	1333	0.706	0.402	0.324
8.0	1250	0.662	0.341	0.268
8.5	1176	0.571	0.266	0.211
9.0	1111	0.429	0.170	0.113
9.5	1053	0.288	0.080	0.055
10.0	1000	0.153	0.013	0.012
10.6	943	0.086	0.006	0.010
11.0	909	0.124	0.040	0.037
11.5	870	0.226	0.093	0.074
12.0	833	0.329	0.153	0.113
12.5	800	0.420	0.205	0.161
13.0	769	0.486	0.236	0.197
13.5	741	0.547	0.277	0.230
14.0	714	0.595	0.311	0.256
14.5	690	0.626	0.343	0.278
15.0	667	0.648	0.362	0.296
15.5	645	0.662	0.377	0.307
16.0	625	0.668	0.391	0.315
16.5	606	0.670	0.394	0.318
17.0	588	0.666	0.396	0.321

Table V

Table of Normalized Experimental Reflectances for Cadmium Selenide
Film Thickness: 2.41 Microns

Wavelength/Wavenumber (microns) (cm ⁻¹)		Incident Angle		
		22 Degrees	51 Degrees	63 Degrees
2.5	4000	0.273	0.126	0.069
3.0	3333	0.099	0.059	0.050
3.5	2857	0.386	0.071	0.018
4.0	2500	0.106	0.054	0.041
4.5	2222	0.398	0.079	0.075
5.0	2000	0.354	0.063	0.023
5.5	1818	0.116	0.000	0.001
6.0	1667	0.127	0.057	0.027
6.5	1538	0.274	0.105	0.059
7.0	1428	0.347	0.117	0.061
7.5	1333	0.344	0.106	0.060
8.0	1250	0.296	0.081	0.052
8.5	1176	0.227	0.054	0.040
9.0	1111	0.158	0.025	0.030
9.5	1053	0.083	0.009	0.023
10.0	1000	0.041	0.003	0.023
10.6	943	0.011	0.003	0.026
11.0	909	0.014	0.008	0.029
11.5	870	0.035	0.014	0.040
12.0	833	0.059	0.026	0.046
12.5	800	0.085	0.043	0.051
13.0	769	0.109	0.054	0.057
13.5	741	0.147	0.061	0.060
14.0	714	0.170	0.071	0.064
14.5	690	0.191	0.080	0.066
15.0	667	0.207	0.086	0.071
15.5	645	0.223	0.091	0.077
16.0	625	0.237	0.099	0.082
16.5	606	0.252	0.105	0.087
17.0	588	0.264	0.113	0.090

Table VI

Table of Normalized Experimental Reflectances for Cadmium Selenide
Film Thickness: 2.59 Microns

Wavelength/Wavenumber (microns) (cm ⁻¹)		Incident Angle		
		22 Degrees	51 Degrees	63 Degrees
2.5	4000	0.344	0.120	0.059
3.0	3333	0.141	0.097	0.058
3.5	2857	0.366	0.046	0.009
4.0	2500	0.127	0.070	0.050
4.5	2222	0.412	0.143	0.074
5.0	2000	0.349	0.063	0.030
5.5	1818	0.113	0.000	0.001
6.0	1667	0.116	0.046	0.024
6.5	1538	0.284	0.097	0.057
7.0	1428	0.374	0.120	0.064
7.5	1333	0.392	0.115	0.061
8.0	1250	0.370	0.101	0.053
8.5	1176	0.309	0.072	0.039
9.0	1111	0.226	0.043	0.018
9.5	1053	0.165	0.014	0.013
10.0	1000	0.092	0.002	0.007
10.6	943	0.053	0.000	0.009
11.0	909	0.051	0.003	0.014
11.5	870	0.064	0.017	0.018
12.0	833	0.091	0.041	0.028
12.5	800	0.134	0.064	0.041
13.0	769	0.176	0.080	0.053
13.5	741	0.207	0.100	0.065
14.0	714	0.247	0.112	0.076
14.5	690	0.274	0.124	0.082
15.0	667	0.292	0.135	0.083
15.5	645	0.305	0.139	0.082
16.0	625	0.311	0.145	0.081
16.5	606	0.315	0.150	0.081
17.0	588	0.315	0.149	0.079

Table VII

Table of Normalized Experimental Reflectances for Cadmium Telluride
Film Thickness: 2.06 Microns

Wavelength/Wavenumber (microns) (cm ⁻¹)		Incident Angle		
		22 Degrees	51 Degrees	63 Degrees
2.5	4000	0.436	0.134	0.063
3.0	3333	0.341	0.187	0.111
3.5	2857	0.259	0.008	0.004
4.0	2500	0.277	0.150	0.098
4.5	2222	0.471	0.182	0.106
5.0	2000	0.318	0.050	0.020
5.5	1818	0.803	0.008	0.008
6.0	1667	0.218	0.101	0.069
6.5	1538	0.383	0.180	0.112
7.0	1428	0.458	0.197	0.122
7.5	1333	0.474	0.192	0.117
8.0	1250	0.456	0.164	0.100
8.5	1176	0.409	0.113	0.072
9.0	1111	0.335	0.073	0.048
9.5	1053	0.230	0.040	0.020
10.0	1000	0.157	0.003	0.009
10.6	943	0.083	0.000	0.002
11.0	909	0.069	0.002	0.006
11.5	870	0.089	0.017	0.014
12.0	833	0.127	0.011	0.034
12.5	800	0.190	0.061	0.049
13.0	769	0.234	0.083	0.057
13.5	741	0.277	0.105	0.072
14.0	714	0.314	0.123	0.083
14.5	690	0.348	0.143	0.094
15.0	667	0.382	0.158	0.101
15.5	645	0.397	0.168	0.107
16.0	625	0.414	0.179	0.112
16.5	606	0.432	0.188	0.113
17.0	588	0.448	0.190	0.114

Table VIII

Table of Normalized Experimental Reflectances for Cadmium Telluride
Film Thickness: 2.09 Microns

Wavelength/Wavenumber (microns) (cm ⁻¹)		Incident Angle		
		22 Degrees	51 Degrees	63 Degrees
2.5	4000	0.473	0.177	0.090
3.0	3333	0.322	0.173	0.103
3.5	2857	0.277	0.012	0.000
4.0	2500	0.285	0.167	0.108
4.5	2222	0.503	0.201	0.126
5.0	2000	0.344	0.074	0.034
5.5	1818	0.088	0.006	0.002
6.0	1667	0.215	0.094	0.062
6.5	1538	0.387	0.180	0.111
7.0	1428	0.468	0.204	0.127
7.5	1333	0.503	0.204	0.123
8.0	1250	0.474	0.183	0.108
8.5	1176	0.430	0.131	0.083
9.0	1111	0.354	0.090	0.053
9.5	1053	0.249	0.045	0.025
10.0	1000	0.173	0.013	0.007
10.6	943	0.091	0.000	0.000
11.0	909	0.070	0.002	0.002
11.5	870	0.088	0.012	0.011
12.0	833	0.127	0.037	0.022
12.5	800	0.190	0.055	0.036
13.0	769	0.235	0.071	0.052
13.5	741	0.273	0.100	0.065
14.0	714	0.309	0.114	0.076
14.5	690	0.351	0.136	0.086
15.0	667	0.377	0.151	0.105
15.5	645	0.400	0.163	0.102
16.0	625	0.419	0.177	0.108
16.5	606	0.437	0.188	0.109
17.0	588	0.450	0.190	0.110

Table IX

Table of Normalized Experimental Reflectances for Zinc Selenide
Film Thickness: 2.06 Microns

Wavelength/Wavenumber (microns) (cm ⁻¹)	Incident Angle		
	22 Degrees	51 Degrees	63 Degrees
2.5	0.087	0.018	0.013
3.0	0.372	0.082	0.037
3.5	0.099	0.063	0.049
4.0	0.396	0.136	0.078
4.5	0.306	0.046	0.015
5.0	0.072	0.002	0.005
5.5	0.182	0.077	0.054
6.0	0.325	0.124	0.082
6.5	0.396	0.143	0.088
7.0	0.392	0.124	0.073
7.5	0.357	0.098	0.055
8.0	0.295	0.060	0.032
8.5	0.223	0.035	0.013
9.0	0.143	0.006	0.002
9.5	0.080	0.000	0.000
10.0	0.063	0.000	0.003
10.6	0.083	0.014	0.012
11.0	0.112	0.031	0.020
11.5	0.163	0.052	0.035
12.0	0.209	0.060	0.046
12.5	0.235	0.079	0.053
13.0	0.272	0.092	0.058
13.5	0.300	0.106	0.066
14.0	0.322	0.117	0.080
14.5	0.344	0.126	0.082
15.0	0.362	0.131	0.083
15.5	0.377	0.134	0.081
16.0	0.388	0.134	0.080
16.5	0.398	0.133	0.076
17.0	0.406	0.134	0.073

Table X

Table of Normalized Experimental Reflectances for Zinc Selenide
Film Thickness: 2.03 Microns

Wavelength/Wavenumber (microns) (cm ⁻¹)		Incident Angle		
		22 Degrees	51 Degrees	63 Degrees
2.5	4000	0.106	0.011	0.011
3.0	3333	0.385	0.089	0.035
3.5	2857	0.100	0.060	0.047
4.0	2500	0.411	0.150	0.082
4.5	2222	0.322	0.053	0.017
5.0	2000	0.079	0.001	0.005
5.5	1818	0.187	0.072	0.053
6.0	1667	0.344	0.126	0.079
6.5	1538	0.413	0.155	0.088
7.0	1428	0.417	0.138	0.076
7.5	1333	0.381	0.106	0.059
8.0	1250	0.431	0.067	0.039
8.5	1176	0.241	0.043	0.015
9.0	1111	0.165	0.006	0.005
9.5	1053	0.089	0.000	0.000
10.0	1000	0.069	0.000	0.006
10.6	943	0.091	0.014	0.009
11.0	909	0.119	0.031	0.018
11.5	870	0.172	0.052	0.034
12.0	833	0.221	0.072	0.046
12.5	800	0.256	0.087	0.055
13.0	769	0.290	0.100	0.058
13.5	741	0.316	0.111	0.060
14.0	714	0.342	0.120	0.062
14.5	690	0.363	0.128	0.062
15.0	667	0.381	0.134	0.062
15.5	645	0.392	0.139	0.062
16.0	625	0.402	0.143	0.060
16.5	606	0.410	0.144	0.060
17.0	588	0.414	0.144	0.060

Table XI

Table of Normalized Experimental Reflectances for Zinc Telluride
Film Thickness: 1.71 Microns

Wavelength/Wavenumber (microns) (cm ⁻¹)		Incident Angle		
		22 Degrees	51 Degrees	63 Degrees
2.5	4000	0.101	0.057	0.054
3.0	3333	0.466	0.111	0.054
3.5	2857	0.302	0.153	0.107
4.0	2500	0.572	0.232	0.146
4.5	2222	0.390	0.063	0.035
5.0	2000	0.105	0.019	0.020
5.5	1818	0.371	0.166	0.106
6.0	1667	0.534	0.230	0.160
6.5	1538	0.577	0.238	0.168
7.0	1428	0.559	0.216	0.139
7.5	1333	0.507	0.174	0.103
8.0	1250	0.410	0.104	0.061
8.5	1176	0.292	0.058	0.027
9.0	1111	0.206	0.012	0.005
9.5	1053	0.118	0.000	0.001
10.0	1000	0.109	0.010	0.010
10.6	943	0.179	0.048	0.034
11.0	909	0.224	0.063	0.052
11.5	870	0.297	0.105	0.065
12.0	833	0.365	0.122	0.087
12.5	800	0.416	0.156	0.103
13.0	769	0.466	0.178	0.115
13.5	741	0.503	0.197	0.127
14.0	714	0.535	0.220	0.138
14.5	690	0.556	0.226	0.150
15.0	667	0.577	0.231	0.159
15.5	645	0.590	0.232	0.165
16.0	625	0.605	0.233	0.173
16.5	606	0.619	0.233	0.173
17.0	588	0.633	0.234	0.176

Table XII

Table of Normalized Experimental Reflectances for Zinc Telluride
Film Thickness: 1.74 Microns

<u>Wavelength/Wavenumber</u> <u>(microns)</u>	<u>(cm⁻¹)</u>	<u>Incident Angle</u>		
		<u>22 Degrees</u>	<u>51 Degrees</u>	<u>63 Degrees</u>
2.5	4000	0.102	0.062	0.049
3.0	3333	0.048	0.110	0.056
3.5	2857	0.306	0.173	0.110
4.0	2500	0.584	0.246	0.173
4.5	2222	0.398	0.075	0.052
5.0	2000	0.102	0.017	0.015
5.5	1818	0.361	0.170	0.109
6.0	1667	0.535	0.235	0.170
6.5	1538	0.579	0.252	0.181
7.0	1428	0.563	0.226	0.153
7.5	1333	0.513	0.184	0.111
8.0	1250	0.419	0.118	0.069
8.5	1176	0.304	0.058	0.036
9.0	1111	0.201	0.012	0.006
9.5	1053	0.122	0.000	0.000
10.0	1000	0.111	0.007	0.006
10.6	943	0.175	0.046	0.026
11.0	909	0.219	0.060	0.048
11.5	870	0.285	0.095	0.063
12.0	833	0.353	0.122	0.084
12.5	800	0.406	0.156	0.102
13.0	769	0.453	0.178	0.112
13.5	741	0.383	0.197	0.128
14.0	714	0.526	0.216	0.140
14.5	690	0.550	0.229	0.154
15.0	667	0.569	0.231	0.162
15.5	645	0.585	0.243	0.168
16.0	625	0.598	0.249	0.175
16.5	606	0.614	0.250	0.178
17.0	588	0.627	0.251	0.178

Table XIII

Table of Normalized Experimental Reflectances for Cadmium Sulfide
Film Thickness: 1.50 Microns

Wavelength/Wavenumber (microns) (cm ⁻¹)		Incident Angle		
		22 Degrees	51 Degrees	63 Degrees
2.5	4000	0.239	0.057	0.022
3.0	3333	0.298	0.063	0.026
3.5	2857	0.226	0.069	0.033
4.0	2500	0.350	0.113	0.057
4.5	2222	0.327	0.069	0.025
5.0	2000	0.194	0.034	0.004
5.5	1818	0.215	0.075	0.045
6.0	1667	0.351	0.130	0.078
6.5	1538	0.431	0.164	0.096
7.0	1428	0.448	0.158	0.088
7.5	1333	0.427	0.126	0.071
8.0	1250	0.380	0.096	0.051
8.5	1176	0.309	0.067	0.023
9.0	1111	0.240	0.038	0.007
9.5	1053	0.195	0.015	0.000
10.0	1000	0.140	0.012	0.000
10.6	943	0.129	0.023	0.009
11.0	909	0.155	0.040	0.023
11.5	870	0.199	0.058	0.042
12.0	833	0.244	0.081	0.054
12.5	800	0.293	0.101	0.067
13.0	769	0.344	0.117	0.079
13.5	741	0.389	0.134	0.097
14.0	714	0.424	0.151	0.111
14.5	690	0.454	0.168	0.121
15.0	667	0.482	0.180	0.122
15.5	645	0.506	0.188	0.124
16.0	625	0.517	0.194	0.127
16.5	606	0.531	0.196	0.127
17.0	588	0.544	0.195	0.126

Table XIV

Table of Normalized Experimental Reflectances for Cadmium Sulfide
Film Thickness: 1.83 Microns

<u>Wavelength/Wavenumber</u>		<u>Incident Angle</u>		
<u>(microns)</u>	<u>(cm⁻¹)</u>	<u>22 Degrees</u>	<u>51 Degrees</u>	<u>63 Degrees</u>
2.5	4000	0.239	0.053	0.011
3.0	3333	0.316	0.091	0.042
3.5	2857	0.189	0.044	0.008
4.0	2500	0.328	0.108	0.059
4.5	2222	0.369	0.094	0.042
5.0	2000	0.212	0.028	0.003
5.5	1818	0.165	0.046	0.018
6.0	1667	0.287	0.098	0.060
6.5	1538	0.397	0.140	0.084
7.0	1428	0.434	0.206	0.087
7.5	1333	0.453	0.192	0.077
8.0	1250	0.400	0.104	0.061
8.5	1176	0.345	0.083	0.043
9.0	1111	0.277	0.054	0.017
9.5	1053	0.214	0.031	0.006
10.0	1000	0.168	0.014	0.000
10.6	943	0.122	0.008	0.002
11.0	909	0.123	0.014	0.005
11.5	870	0.157	0.014	0.014
12.0	833	0.196	0.049	0.029
12.5	800	0.236	0.060	0.044
13.0	769	0.281	0.075	0.054
13.5	741	0.327	0.094	0.065
14.0	714	0.366	0.112	0.092
14.5	690	0.402	0.126	0.095
15.0	667	0.429	0.139	0.096
15.5	645	0.447	0.146	0.099
16.0	625	0.465	0.154	0.101
16.5	606	0.485	0.157	0.102
17.0	588	0.498	0.158	0.102

Table XV

Table of Normalized Experimental Reflectances for Potassium Chloride

Wavelength/Wavenumber (microns) (cm ⁻¹)		Incident Angle		
		22 Degrees	51 Degrees	63 Degrees
2.5	4000	0.060	0.000	0.000
3.0	3333	0.061	0.001	0.001
3.5	2857	0.062	0.002	0.002
4.0	2500	0.065	0.003	0.002
4.5	2222	0.064	0.003	0.004
5.0	2000	0.065	0.000	0.004
5.5	1818	0.065	0.002	0.004
6.0	1667	0.065	0.006	0.004
6.5	1538	0.065	0.008	0.004
7.0	1428	0.065	0.012	0.004
7.5	1333	0.066	0.009	0.004
8.0	1250	0.066	0.009	0.004
8.5	1176	0.067	0.006	0.004
9.0	1111	0.069	0.003	0.006
9.5	1053	0.065	0.002	0.006
10.0	1000	0.068	0.001	0.006
10.6	943	0.069	0.000	0.006
11.0	909	0.071	0.002	0.006
11.5	870	0.071	0.002	0.006
12.0	833	0.070	0.003	0.006
12.5	800	0.071	0.005	0.006
13.0	769	0.071	0.008	0.007
13.5	741	0.070	0.008	0.007
14.0	714	0.070	0.009	0.007
14.5	690	0.072	0.014	0.007
15.0	667	0.072	0.016	0.007
15.5	645	0.075	0.019	0.007
16.0	625	0.076	0.023	0.007
16.5	606	0.079	0.023	0.007
17.0	588	0.085	0.025	0.007

Appendix C

Tables of Maxima and Minima in the Reflection Spectra

The following tables show the wavenumbers where the maxima and minima occurred in the experimental reflection spectra. The wavenumbers where each maximum and minimum occurred were recorded for each spectrum and then averaged for coatings of the same thickness. Each table is arranged so that the average maxima and minima for both thicknesses of a thin film coating are shown at each incident angle.

Table XVI

Table of Reflectance Maxima and Minima for Zinc Sulfide

Thickness	2.71 Microns		2.65 Microns	
Incident Angle	Maxima (cm ⁻¹)	Minima (cm ⁻¹)	Maxima (cm ⁻¹)	Minima (cm ⁻¹)
22 Degrees	3070	3500	3830	3415
	2190	2620	2980	2570
	1335	1755	2140	1733
	620	905	1315	898
51 Degrees			623	
	3300	3740		3540
	2340	2810	3110	2670
	1435	1890	2220	1810
63 Degrees	655	965	1370	920
			635	
	3360	3840		3630
	2370	2900	3185	2725
	1480	1930	2295	1820
	685	980	1393	953
			670	

Table XVII

Table of Reflectance Maxima and Minima for Germanium

Thickness	1.27 Microns		1.33 Microns	
Incident Angle	Maxima (cm^{-1})	Minima (cm^{-1})	Maxima (cm^{-1})	Minima (cm^{-1})
22 Degrees	3265	3725	3260	3710
	2315	2815	2320	2805
	1428	1895	1420	1888
	603	955	593	950
51 Degrees	3330	3780	3310	3760
	2370	2860	2370	2850
	1430	1925	1435	1915
		970		965
63 Degrees	3340	3805	3335	3795
	2400	2880	2380	2870
	1455	1943	1458	1930
		973		973

Table XVIII

Table of Reflectance Maxima and Minima for Cadmium Selenide

Thickness	2.41 Microns		2.59 Microns	
Incident Angle	Maxima (cm ⁻¹)	Minima (cm ⁻¹)	Maxima (cm ⁻¹)	Minima (cm ⁻¹)
22 Degrees	3780	3380	3835	3420
	2960		2990	
	2140		2155	
	1390		1340	
			570	
51 Degrees	3940	3520	3150	3610
	3080		2260	
	2230		1395	
	1430		590	
63 Degrees	3120	3590	3195	3655
	2260		2260	
	1430		1410	
			640	

Table XIX

Table of Reflectance Maxima and Minima for Cadmium Telluride

Thickness	2.06 Microns		2.09 Microns	
Incident Angle	Maxima (cm ⁻¹)	Minima (cm ⁻¹)	Maxima (cm ⁻¹)	Minima (cm ⁻¹)
22 Degrees	3130	3570	3105	3550
		2675		2680
	2215	1795	2205	1788
	1338	908	1338	905
	550		555	
51 Degrees	3260	3730	3230	3670
		2790		2790
	2330	1880	2300	1850
	1415	950	1385	925
	540		540	
63 Degrees	3295	3755	3275	3700
		2810		2825
	2340	1880	2335	1875
	1430	940	1403	938
	580		565	

Table XX

Table of Reflectance Maxima and Minima for Zinc Selenide

Thickness	2.06 Microns		2.03 Microns	
Incident Angle	Maxima (cm ⁻¹)	Minima (cm ⁻¹)	Maxima (cm ⁻¹)	Minima (cm ⁻¹)
22 Degrees	3420	3920	3420	3910
		2935		2930
	2420	1965	2400	1963
	1493	998	1480	990
	473		585	
51 Degrees	3590	3070	3570	3050
	2560	2050	2560	2030
	1560	1045	1535	1040
	610		590	
63 Degrees	3650	3110	3610	3110
	2600	2090	2570	2070
	1570	1055	1555	1048
	663		670	

Table XXI

Table of Reflectance Maxima and Minima for Zinc Telluride

Thickness	1.71 Microns		1.74 Microns	
Incident Angle	Maxima (cm ⁻¹)	Minima (cm ⁻¹)	Maxima (cm ⁻¹)	Minima (cm ⁻¹)
22 Degrees	3535	3035	3520	3030
	2495		2500	
	1535		1523	
	600		585	
51 Degrees	3620	3120	3620	3120
	2600		2590	
	1560		1540	
	570		560	
63 Degrees	3665	3150	3660	3150
	2600		2610	
	1570		1578	
	563		560	

Table XXII

Table of Reflectance Maxima and Minima for Cadmium Sulfide

Thickness	1.80 Microns		1.83 Microns	
Incident Angle	Maxima (cm ⁻¹)	Minima (cm ⁻¹)	Maxima (cm ⁻¹)	Minima (cm ⁻¹)
22 Degrees	3395	2925 1938 963	3290 2325 1390 583	3790 2820 1878 928
	2395			
	1440			
	593			
51 Degrees	3580	3060 1990 1020	3430 2420 1460 560	2920 1960 960
	2500			
	1500			
	590			
63 Degrees	3585	3115 2015 1035	3480 2470 1460 580	2975 1960 968
	2530			
	1520			
	585			

Appendix D

Computed Indices of Refraction

This appendix contains the indices of refraction, n , calculated for each material using equation (26) and the information from the reflection spectra. It would have been better if the information could have been presented graphically instead of in a table. However, there were only six fringes for each sample, which resulted in only six data points for a graph. Another problem was that the calculated indices were normally not consistent with one another. Therefore, it seemed better to present them in a tabular form with the applicable wavelength regions indicated. The following paragraphs explain how the tables were constructed.

In each spectrum there normally were six fringes; three fringes going from amplitude maximum to amplitude maximum, and three fringes going from amplitude minimum to amplitude minimum. An n was calculated for each single fringe to obtain an idea of how n changed as wavelength increased. This was necessary since equation (26) only gives an average n over the $\Delta\lambda$ used.

The fringes occurred at about the same wavelength for each incident angle, so an n for each corresponding fringe at each incident angle was calculated. Then the three n 's were averaged to obtain the n presented in the following tables. To obtain the wavelength range for an averaged n , the wavelengths for the beginning and end of the three corresponding fringes were averaged. This introduced an error of $\pm 0.1\mu$ in the shorter wavelengths and $\pm 0.4\mu$ in the longer wavelengths.

Occasionally only one of the three spectra for a given sample would have a complete fringe at the beginning or end of a spectrum, due to the different incident angles. When this occurred, the one fringe was used to calculate n for that wavelength range, and no averaging was involved. Those values of n are marked by an asterisk in the following tables.

Table XXIII

Computed Indices of Refraction for Zinc Sulfide

<u>Type Fringe Used to Obtain Δv</u>	<u>Measured Film Thickness (microns)</u>	<u>Average n</u>	<u>From (microns)</u>	<u>To (microns)</u>
Maximum to Maximum	2.71	2.09	3.1	4.3
		2.21	4.3	7.1
		2.42	7.1	15.3
Maximum to Maximum	2.65	2.28	3.2	4.5
		2.31	4.5	7.4
		2.73	7.4	15.6
Minimum to Minimum	2.71	2.14	2.7	3.6
		2.14	3.6	5.4
		2.16	5.4	10.5
Minimum to Minimum	2.65	2.28	2.8	3.8
		2.30	3.8	5.6
		2.30	5.6	10.8

Table XXIV

Computed Indices of Refraction for Germanium

<u>Type Fringe Used to Obtain Δv</u>	<u>Measured Film Thickness (microns)</u>	<u>Average n</u>	<u>From (microns)</u>	<u>To (microns)</u>
Maximum to Maximum	1.33	4.04	3.0	4.2
		4.15	4.2	11.0
		4.56*	11.0	16.9
Maximum to Maximum	1.27	4.20	3.0	4.2
		4.34	4.2	7.0
		4.79*	7.0	16.6
Minimum to Minimum	1.33	4.18	2.7	3.5
		4.11	3.5	5.2
		4.03	5.2	10.4
Minimum to Minimum	1.27	4.35	2.7	3.5
		4.29	3.5	5.2
		4.19	5.2	10.4

Table XXV

Computed Indices of Refraction for Cadmium Selenide

<u>Type Fringe Used to Obtain Δv</u>	<u>Measured Film Thickness (microns)</u>	<u>Average n</u>	<u>From (microns)</u>	<u>To (microns)</u>
Maximum to Maximum	2.59	2.30	3.2	4.5
		2.40	4.5	7.2
		2.57	7.2	16.7
Maximum to Maximum	2.41	2.55	2.6	3.3
		2.59	3.3	4.5
		2.75	4.5	7.1
Minimum to Minimum	2.59	2.30	2.8	3.7
		2.32	3.7	5.6
		2.38	5.6	10.5
Minimum to Minimum	2.41	2.52	2.9	3.8
		2.64	3.8	5.5
		2.55	5.5	10.3

Table XXVI

Computed Indices of Refraction for Cadmium Telluride

<u>Type Fringe Used to Obtain Δv</u>	<u>Measured Film Thickness (microns)</u>	<u>Average n</u>	<u>From (microns)</u>	<u>To (microns)</u>
Maximum to Maximum	2.09	2.68	3.1	4.4
		2.75	4.4	7.3
		3.00	7.3	18.1
Maximum to Maximum	2.06	2.70	3.1	4.4
		2.79	4.4	7.2
		2.99	7.2	17.9
Minimum to Minimum	2.09	2.63	2.7	3.6
		2.68	3.6	5.4
		2.71	5.4	10.8
Minimum to Minimum	2.06	2.72	2.7	3.6
		2.77	3.6	5.4
		2.78	5.4	10.7

Table XXVII

Computed Indices of Refraction for Zinc Selenide

<u>Type Fringe Used to Obtain Δv</u>	<u>Measured Film Thickness (microns)</u>	<u>Average n</u>	<u>From (microns)</u>	<u>To (microns)</u>
Maximum to Maximum	2.06	2.47	2.8	4.0
		2.57	4.0	6.5
		2.72	6.5	16.3
Maximum to Maximum	2.03	2.51	2.8	4.0
		2.61	4.0	6.5
		2.81	6.6	16.3
Minimum to Minimum	2.06	2.49	2.6	3.3
		2.52	3.3	4.9
		2.53	4.9	9.7
Minimum to Minimum	2.03	2.54*	2.6	3.3
		2.55	3.3	4.9
		2.58	4.9	9.7

Table XXVIII

Computed Indices of Refraction for Zinc Telluride

<u>Type Fringe Used to Obtain Δv</u>	<u>Measured Film Thickness (microns)</u>	<u>Average n</u>	<u>From (microns)</u>	<u>To (microns)</u>
Maximum to Maximum	1.74	2.87	2.8	3.9
		2.91	3.9	6.5
		3.03	6.5	17.6
Maximum to Maximum	1.71	2.90	2.8	3.9
		2.99	3.9	6.4
		3.08	6.4	17.3
Minimum to Minimum	1.74	2.81	3.2	4.9
		2.92	4.9	9.7
Minimum to Minimum	1.71	2.89	3.2	4.9
		2.97	4.9	9.6

Table XXIX

Comput Indices of Refraction for Cadmium Sulfide

<u>Type Fringe Used to Obtain Δv</u>	<u>Measured Film Thickness (microns)</u>	<u>Average n</u>	<u>From (microns)</u>	<u>To (microns)</u>
Maximum to Maximum	1.83	2.83	2.9	4.2
		2.92	4.2	7.0
		3.26	7.0	17.4
Maximum to Maximum	1.80	2.76	2.8	4.0
		2.90	4.0	6.7
		3.18	6.7	17.0
Minimum to Minimum	1.83	2.84*	2.6	3.4
		2.90	3.4	5.2
		2.88	5.2	10.5
Minimum to Minimum	1.80	-	-	-
		2.74	3.3	5.0
		2.93	5.0	9.9

Appendix E

Flow Chart of Computer Program

The following figure is a flow chart of a computer program written to analyze a reflectance spectrum of a thin film on a substrate at any wavelength. The program, by an iterative process, obtains the extinction coefficient of the film, k , for any given index of refraction of the film, n . The initial value of n is read on a data card. The value of n varies from its initial value to its initial value plus 1.0, in 0.1 increments.

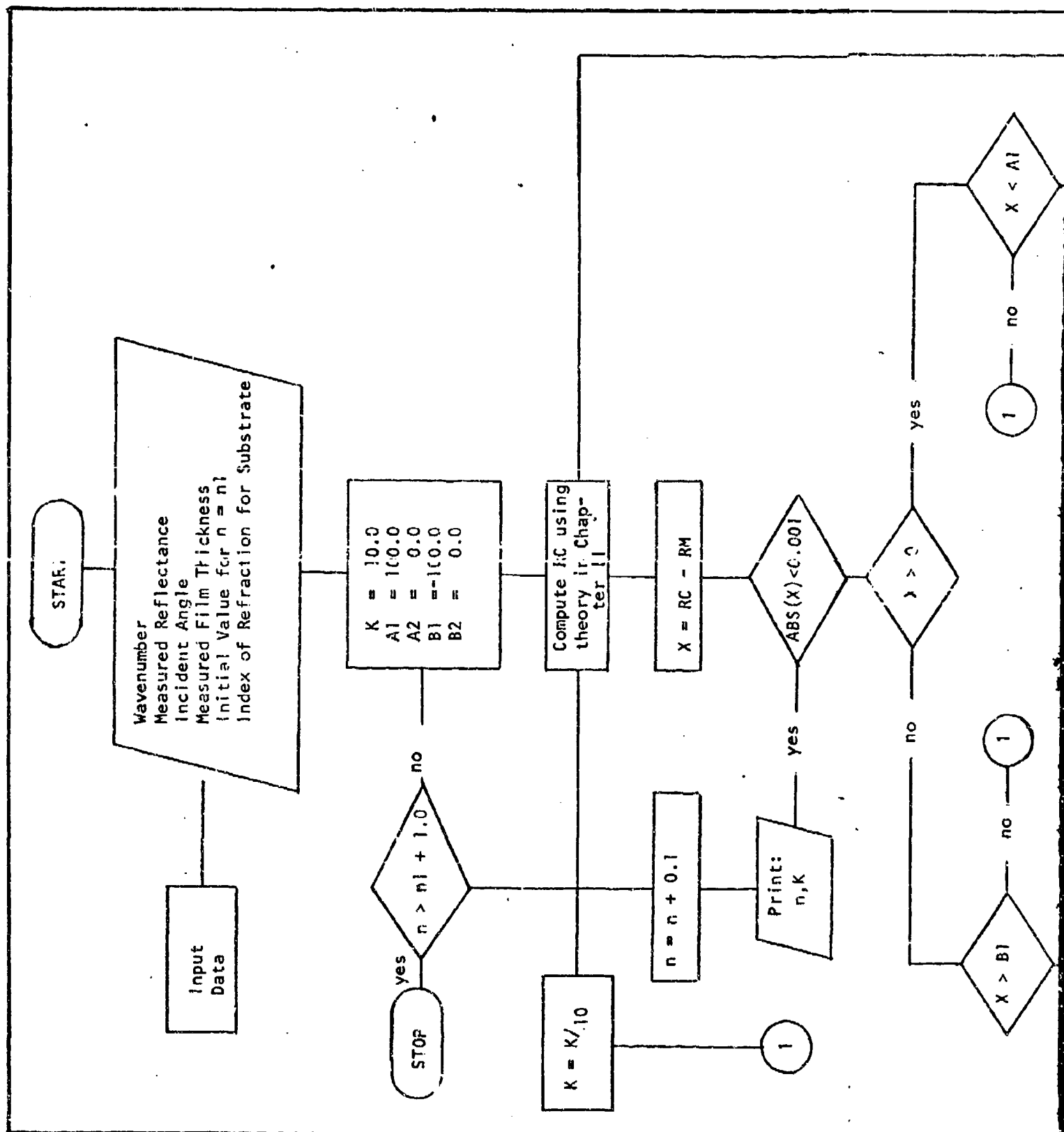
With the information read on a data card and the equation (20) developed in Chapter II, a reflectance is computed. Then the difference between the computed reflectance and the normalized measured reflectance is calculated. If the absolute value of the difference is greater than 0.001, a new k is calculated and another reflectance is computed using the new k . This iteration process continues until the difference between the computed and measured reflectance is less than 0.001. When the difference becomes less than 0.001, 0.1 is added to n and the process starts over to find a k to satisfy equation (20) for the new n . This process continues until the range of n values is exhausted.

The flow chart is straight forward until the iteration process for k is reached. The iteration process is based on the assumption that for any given n value, there exists a k_1 value that will give a computed reflectance greater than the measured reflectance, and there exists a k_2 value that will give a calculated reflectance less than

the measured reflectance. The program then finds a k value halfway between k_1 and k_2 and uses the new k to compute a new reflectance, which should bring the computed reflectance closer to the measured reflectance.

The symbols used in the flow chart are defined below.

RC	=	computed reflectance
RM	=	normalized measured reflectance
X	=	storage address for the difference between RC and RM
A1	=	storage address for $X > 0$
A2	=	storage address for k 's which result in $X > 0$
B1	=	storage address for $X < 0$
B2	=	storage address for k 's which result in $X < 0$
n	=	index of refraction of the film
k	=	extinction coefficient of the film



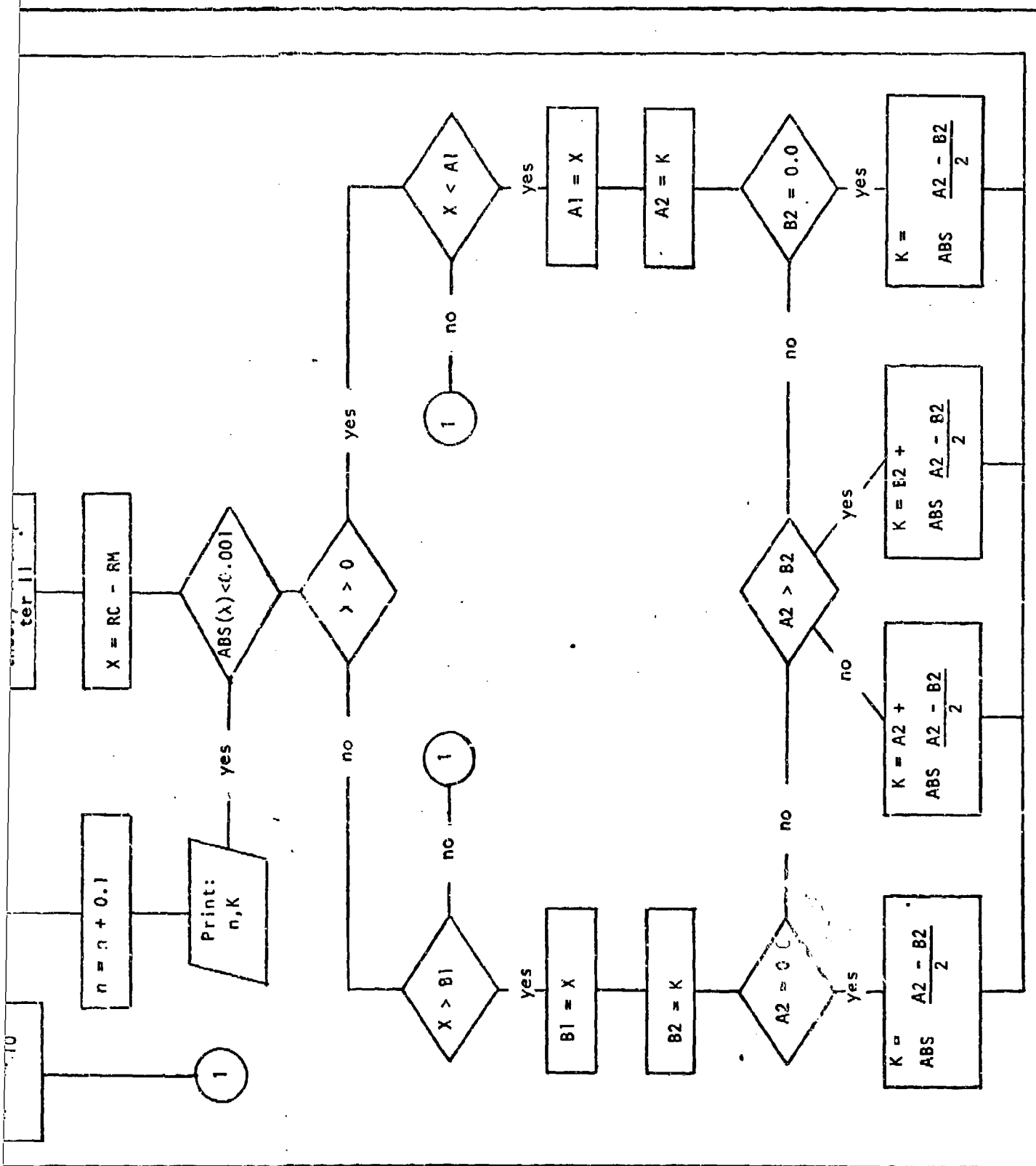


Fig.13. Flow Chart of Computer Program

VITA

Jan B. Jaeger was born on 26 April 1944 in Vermillion, South Dakota. He moved to Washington State in 1954 and graduated from high school in Mt Vernon, Washington in 1962. He graduated from the United States Air Force Academy in 1966 and received a Bachelor of Science degree in Civil Engineering. After flying training, he was assigned to the 558th Tactical Fighter Squadron, Cam Ranh Bay, Republic of Vietnam. After this tour, he returned to Laredo AFB, Texas, where he served as an Instructor pilot for three years. He attended the Air Force Institute of Technology where he received a Master of Science in Engineering Physics in 1974.

Permanent address: 2908 Mt. Baker Hiway
Bellingham, Washington 98225

This thesis was typed by Mrs. Barbara D. Rice.